

Shifting Perception: Adaptation to a Curvature Gain in Redirected Walking

Niklas Stein

April 9, 2019



Westfälische Wilhelms-Universität Münster

Department 7 - Psychology & Sports Sciences

First Examiner: Prof. Dr. Markus Lappe

Second Examiner: Dr. Annegret Meermeier

Niklas.Stein@wwu.de

Klosterstraße 40

48143 Münster

Matriculation number: 407577

Contents

Using Redirected Walking in Virtual Reality	5
Point & Teleport	6
Redirected Walking	7
Rotational Gains	8
Translational Gains	9
Curvature Gains	9
RDW Algorithms	10
Hypotheses	12
Method	14
Subjects	14
Experimental Setup	14
Experimental Procedure	16
Straight Walking & Pointing Task	17
Threshold Measurement	17
Instructional Block	22
Adaptation	22
Curvature Gain	22
Statistical Tests	23
Results	25
Tracking Data	25
Pointing Task	25
Straight Walking Task	25

ADAPTATION TO A CURVATURE GAIN	3
Adaptation	29
Threshold Measurement	29
Perceptual Thresholds	31
Orientation Tracking	38
Questionnaires	39
Discussion	41
Hypotheses	41
Limitations	43
Adaptation to Complex Algorithms	43
The Influence of Walking Speed	44
Fitting of the Psychometric Curves	44
Pointing Task	44
Orientation Data	45
Prospects	46
References	48
Appendix	55
A1: Instructions	55
A2: Curvature Gain	59
A3: Straight Walking & Pointing Task	60
A4: Threshold Measurement	61
Acknowledgements	67
Plagiatserklärung	68

Abstract

Virtual Reality (VR) allows perceiving a programmed world without physical limitations. In this study, 12 subjects (4 female) were adapted to a Redirected walking (RDW) technique that can be used to imperceptibly maximize the use of limited physical tracking space. The applied curvature gain forced subjects to walk along a curve in the physical world, to walk in a straight line in VR, since the virtual environment (VE) was continuously rotated depending on their position in the room. In 3 experimental sessions on 3 subsequent days, the perceived walking direction was measured with a 2AFC-like task for 7 different curvature gains. In the second experimental session, a constant curvature gain of $\frac{\pi}{30}$ was applied for 20 minutes. After the adaptation phase, the perceptual threshold shifted. Moreover, when walking without visual feedback in a straight line after the adaptation, subjects walked in a curve. Threshold measurements were repeated in experimental session 3 and carry-over effects were found. The results can be used to enhance RDW algorithms for maximizing the use of the available physical space.

Using Redirected Walking in Virtual Reality

During the last decade, the complexity and graphical detail of virtual environments (VE) has evolved dramatically. Today, the graphical output of head mounted displays (HMD) can be presented in high-definition and position tracking systems are used in entertainment and gaming applications all over the world. Also the needed soft- and hardware became much cheaper and easier to handle. Therefore, high hopes were set in the application of virtual reality (VR) in different scenarios. Inspired by the possibility to include tracked natural movements like walking, VR offers interesting tools for motoric learning. One possibility is to transfer realistic tasks into a VE in order to train the handling of the specific situation in a safe space and at lower costs. Additionally, it is possible to decouple visual information from the motoric feedback of the body, which allows to examine their relationship. On the long term, this may help to understand the processing of visual and proprioceptional information during motoric learning. Moreover, decoupling can be used to create scenarios that may help to train specific motoric skills of persons, who are hindered by the visual input in the real (e.g. a rehabilitation program that has been proven to be an effective possibility to extend the movement range of chronic back-pain patients (Bolte, de Lussanet, & Lappe, 2016)).

Since walking is the most natural way of moving in the real world, it is highly desirable to allow the same locomotion in a realistic VR setting. This goal can be achieved by position tracking of the HMD, hands and feet and the possibility of modern VR engines to manipulate the visual output according to the tracked movements. But in most cases the tracked walking area is limited to a room-sized physical space. If one is interested in exploring bigger areas, different techniques must be used, of which some also include decoupling to a certain extend.

Point & Teleport

In recent VR applications, a locomotion technique called Point & Teleport became more popular (Bozgeyikli, Raij, Katkooori, & Dubey, 2016). To change the position in the VE, the user points at a specific location and then triggers a teleport by pressing a button on the controller. The original direction of orientation stays the same. To achieve a more natural feeling, in some recent games like Portal Stories: VR (Prism Game Studios Ltd., 2016), mixtures of Point & Teleport and natural walking are used. One can walk to overcome small distances in a tracked area and teleport at positions, which are further away. Since the users orientation is not manipulated during the teleportation, this, of course means that it is still possible to reach the physical limits of the tracked area, while one is walking. In that case, the VE needs to be reset.

Additionally, Point & Teleport might not be applicable in some scenarios. Whenever specific motoric movements (e.g. going to a visual target in great height) shall be learned and transferred into a real world setting afterwards, it should be considered that motor adaptation and learning are driven by the sensory prediction error between the actual and the planned behaviour (Shadmehr, Smith, & Krakauer, 2010). Skipping the calibration process by teleporting and therefore, not performing the walking movement might not be a desirable solution, as it might initiate a completely different process: All movements that include translation, when the same task should be performed in a real world setting, may require relearning. On the other hand, a scenario that is allowing the performance of natural movements is likely to allow an easier transfer to the real world. Lastly, because Point & Teleport does not occur in contexts apart from VR, it is likely that it needs more cognitive resources than natural walking. The explicit action and its handling has to be learned before achieving locomotion. This might be perceived as hindering when using

a VR application for the first time. Moreover, Point & Teleport may lead to a lower performance in VE with complex tasks. Already in 1997 results of Bowman et al. suggest that spatial awareness is worse, when using Point & Teleport, compared to evolving locomotion techniques. Accordingly, Larrue et al. (2014) found that distance estimates were improved when a realistic translation was included, compared by a condition in which translation was achieved with a joystick. Moreover, subjects performed best in a way-finding task, when they were able to perform translational movements including self-rotation.

Redirected Walking

Another solution to maximize the limited area are multiple techniques known as redirected walking (RDW) that were described first by Razzaque, Kohn, and Whitton in 2001. Since small differences between one's motoric perception and the visual input are not detected by the user, a VE can be manipulated to imperceptibly change the user's walking path.

To make best use of this effects, principles of multisensoric integration are taken into account: Visual motion and self-movement are perceived as an integrated percept, while they systematically depend on each other. In comparison to the real world, it is possible to decouple them in VR, by changing the visual input that is presented on the HMD. If both percepts are apparently unfitting (e.g. when someone else's movements are presented), the two sources of perception are hard to integrate. Often this leads to balance issues, slower movements and other symptoms of motion sickness. In RDW, the visual input is not fully decoupled, but slightly manipulated in a systematic way. Instead of changing the visible input completely, the anticipated and appropriate movements are scaled by a factor (gain). This approach can be used in different ways that can be seen in Figure 1.

Rotational Gains. One possibility to redirect the walking path of a user in VR is to manipulate rotation angles. While the original direction of the physical rotation stays the same, its angle is changed (e.g. when a gain $gR = 2$ is applied, a rotation of 90° in the real world is extended to a rotation of 180° in the VE). The threshold at which subjects perceive the manipulation is defined as the gain at which it is possible to detect the redirection with a probability of 75% in a 2AFC-like task.

Perceptual thresholds of rotational gains were tested in different studies: Steinicke et al. found a lower threshold of .88. and even at a gain of 0.77 only 11% of the subjects were able to recognize the manipulation. The complete distribution towards lower rotational gains can be found in Steinicke et al. (2009), Figure 4 C. In a different study, an upper threshold at a gain of $gR = 1.24$ and a lower threshold at a gain of $gR = 0.67$ was found (Steinicke, Bruder, Jerald, Frenz, & Lappe, 2010). Later on, Bruder, Interrante, Phillips, and Steinicke (2012) confirmed these thresholds with findings of $gR = 1.26$ and $gR = 0.68$. A previous study found similar thresholds for a virtual angle of 10° , but also much smaller values when doing the same experiment with higher virtual angles (e.g. 180° : $gR = 0.83$ and $gR = 1.16$). Thus, the threshold is dependent on the size of the rotational angle (Bruder, Steinicke, Hinrichs, & Lappe, 2009). Jerald, Whitton, and Brooks (2012) found that perceptual thresholds are greater when the VE moves along with the head rotation ($gR = 1.11$) in comparison to when the VE moves against the movement of the head ($gR = 1.05$). Additionally, Peck, Fuchs, and Whitton (2009) found that the ranges of rotational gains can be further increased by adding distractors to the VE. All in all, even if one assumes conservative detection thresholds of $gR = 0.80$ and $gR = 1.2$, this would mean that a rotation of 90° can be decreased to 72° and increased to 108° , without the user noticing.

Translational Gains. When using translational gains, a scaling factor is applied to the moving distance of a subject in a specific direction. Comparable to the myth of *The Seven-League Boots*, users can translate through the VE with larger steps, when a translational gain is used. E.g. with a gain of $gT = 2$, a locomotion of 1 m in the real world is extended to a movement of 2 m in the VE, although it makes sense to increase the gain during the movement, instead of using a fixed gain, to create a more natural experience (Interrante, Ries, & Anderson, 2007; Williams et al., 2006). In 2010, Steinicke et al. measured detection thresholds for translational gains for fixed gains of 1.07 and 0.86. This means, by applying translational gains, a virtual distance of 10 m could be extended to 10.7 m or decreased to 8.6 m without the user noticing.

Curvature Gains. Curvature gains are used to lead the user imperceptibly onto a curve during forward movements. The effect can be achieved by successively increasing an orientation angle that is added to the perspective of the HMD, dependent on the position in physical space. Taking the physical forward movements into account, the virtual world is turning leftwards around the subject. Accordingly, subjects have to walk in a rightward curve in the physical space to correct the orientation angle and walk in a straight line in the VE. The size of a curvature gain is defined by the radius of the curve on which the user should be led. Hence big radii imply less redirecting. Ultimately, this approach makes it possible to experience an unlimited VE, while staying within a limited physical space. In the past, multiple studies investigated the perceptual threshold for curvature gains: After Steinicke et al. (2010) had found a threshold at the radius of 22.03 m, Grechkin, Thomas, Azmandian, Bolas, and Suma (2016) detected even smaller values of 11.6 m and 6.4 m noting that the estimation method of Steinicke might be too conservative. Moreover, they proved that translational gains did not affect the curvature

gain detection. Nogalski and Fohl (2017) however, assumed that the measured curvature gains underestimate the necessary physical space because redirected subjects were not always walking on the ideal circular path. In 2012, Neth et al. could reduce the threshold to approximately 10 m, by slowing down the walking speed of subjects to 0.75 m/s. Nguyen, Rothacher, Lenggenhager, Brugger, and Kunz (2018) replicated the influence of speed and discovered an effect of gender. According to their study men (10.7 m) were more sensitive to curvature redirection than woman (8.63 m). But they also noted that the variance between both groups was still quite high and assumed that visual dependence might be a better predictor than gender. Langbehn, Lubos, Bruder, and Steinicke (2017) applied curvature gains on curved virtual paths to further increase their bending in the same direction (see Figure 1 D). They found that they could imperceptibly decrease a virtual radius of 10.88 m to 2.5 m in physical space .

RDW Algorithms. To achieve an unlimited VE, multiple RDW techniques can be combined to build more complex algorithms that also include the movements and position of the user. Additional to the techniques presented, it is possible to manipulate the VE even when the user is not moving. This has been achieved by using effects like change blindness (Suma et al., 2011), saccadic suppression (Bolte & Lappe, 2015; Sun et al., 2018) and eye blinks (Langbehn & Steinicke, 2018), but the eye trackers needed for the application of this ideas are still very expensive. When RDW was introduced in 2001, Razzaque et al. already used rotational gains that were changing according to the next predefined waypoints in the experiment.

The idea of so-called Steer to Center algorithms is to choose the best RDW technique for the current situation and continuously, try to steer the user to the center of the physical space, in order to reduce situations in which the limits of the tracking space are

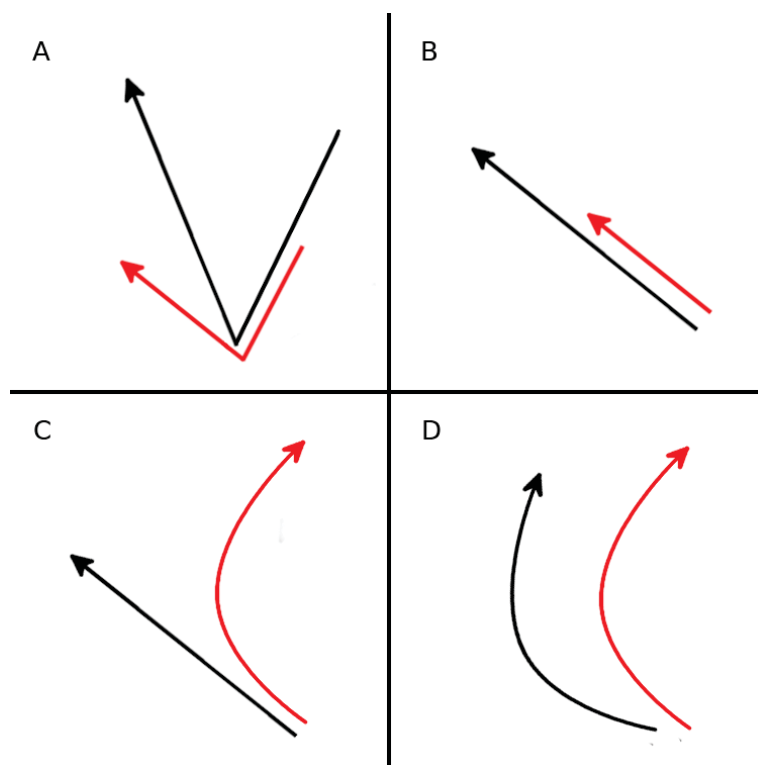


Figure 1. Overview of different methods in RDW. Red arrows show physical paths, the virtual paths are shown in black. A) Rotational gain < 1 . B) Translational gain > 1 . C) Curvature gain rightwards. D) Rightward curvature gain applied on a curved virtual path.

reached (Peck, Whitton, & Fuchs, 2008). In 2008, Hodgson et al. implemented a Steer to Center algorithm and could even show that it did not impact the memory for spatial locations and landmarks. Later on, Nescher, Huang, and Kunz (2014) presented their predictive control algorithm that could significantly reduce the needed redirections.

Regarding the cognitive load of RDW, Bruder, Lubos, and Steinicke (2015) found that redirecting influences verbal as well as spatial working memory tasks. Moreover, an effect of cognitive tasks on the walking behaviour could be shown.

Hypotheses

To maximize the effects of RDW, it is desirable to use strong curvature gains to decrease the physical space, which would be necessary. Additionally, the VE needs to feel natural to the user, so all applied manipulations should be below the perceptual threshold. Since motor functions of the brain have proven to adapt flexibly to their environment by fulfilling different tasks (e.g. eye movements (Hopp & Fuchs, 2004) or reaching tasks (Tseng, Diedrichsen, Krakauer, Shadmehr, & Bastian, 2007)), the same principle might be sufficient to manipulate the perception of curvature gains. According to this idea, the subjects' motor action should adapt to automatically reduce the perceived error. This adaptation process might not only change the perception of the curvature gain, but moreover, change the walking behaviour according to the gain. If the representation of the pointing direction is also influenced by the process, adaptation should even worsen the performance of pointing at a visual target. Until now, there is no study that investigated these questions for VR applications. It is also unknown how long possible adaptation effects to RDW can persist. For eye movements, it is known that an saccadic adaptation effect can be measured even 19 days after the exposure (Alahyane & Pélisson, 2005). To test the proposed effects of an adaptation to a VE with a constant curvature gain, three different tasks were designed and run on three consecutive days, resulting into the following hypotheses:

- H1:** The exposure to a constant rightward curvature gain for 20 minutes results in an increased perceptual threshold for rightward curvature gains.
- H2:** After adaptation to a rightward curvature gain, subjects walk in a rightward curve when asked to walk in a straight line, without visual feedback.

H3: After adaptation to a rightward curvature gain, subjects point to the right when asked to point straight at a target, without visual feedback.

H4: Changes of the perceptual threshold persist even one day after the adaptation.

Method

Subjects

Twelve participants (8 male, 4 female) took part in the study and completed the full set of three sessions. All participants were students or members of the Department of Psychology of the Westfälische Wilhelms-Universität Münster, ranging in age from 20 to 38 years (mean age 25 years). All subjects had normal or corrected-to-normal vision, no history of visual or motor problems and gave written informed consent to the participation on the study. The experimental procedures were approved by the Ethics Committee of the Westfälische Wilhelms-Universität Münster.

Experimental Setup

The experiments were conducted in the VR laboratory of the psychological institute of the Westfälische Wilhelms-Universität Münster, in a tracked area of 10.6 m × 6 m. The VE was presented on an Oculus Rift CV1 HMD with a nominal field of view of 110° and a resolution of 1080 x 1200 pixels per eye. The HMD was used with the thin inlay-version by the manufacturer. The view of the custom-made scene was presented in the HMD depending on head position and orientation. We chose to use a desert as VE because we wanted the environment to be natural enough to create immersion, but also somehow generic, so rotational changes between trials were less likely to be detected. Stimuli were presented with a MSI GE63VR 7RF Raider notebook using Unity 2017.4.3f1 (Unity Technologies, 2017). User input was recorded with a Macally Airstick that was equipped with a LED that could be tracked by the optical tracking system. During the measurements, participants wore a backpack, in which the notebook and two batteries were carried. The experimenter was able to monitor the experiment through a remote desktop connection to the notebook via WiFi. The head position was tracked

with an active optical tracking system (Precise Position Tracking (PPT) manufactured by WorldViz) with an update rate of 90 Hz on a Dell Dimension 8300 computer with an Intel Pentium 4 CPU with 2.8GHz and 240 MB of RAM running Microsoft Windows XP Home Edition (SP1) and PPT Studio by WorldViz (Version 3.21.5791) with four cameras. The raw position data of two LEDs that were fixed to the HMD with a distance of 40 cm was sent to the notebook in the backpack via WiFi. It was then imported with a VRPN plug-in in our custom-made software. The mean position of the head was calculated correcting for the position of the LEDs on the HMD. This signal was then filtered using a Kalman filter (1960).

If only one or no LED could be tracked, the experiment was paused and a red mask appeared on the HMD. Every time the two LED positions were updated, a custom filter checked, whether the distance between each other was less than 60 cm. If this was not the case, the experiment was paused and the red mask appeared as well. In case a position closer than 30 cm to the walls of the physical room was reached, a fence, indicating the size of the room, appeared in the VE.

During pretesting the experiment, we noticed that the orientation data of the gyroscopic sensors of the HMD and the orientation data of the optical tracking system diverged over time. Since an alignment of both systems was crucial to conduct the experiment, we decided to reset the HMD orientation after every trial. To measure the error, the differences of 50 data points that were gathered when subjects were tracked between 1 m and -1 m in y-direction around the center of the VE, were averaged. Additionally, it was checked if the vector resulting from both LEDs changed more than 90° from one tracked position to another. In this case, we assumed that the tracking system lost track of the LEDs and initialized them the wrong way round and corrected the gathered data

for this error, so subjects were not realigned with an error of 180° . Moreover, we decided to add an InertiaCube 3 (InterSense) with an update rate of 180 Hz that was fixed on the front side of the HMD. Although the data of the second sensor was not used for orientation tracking it was imported into the custom-made software in real-time to allow a comparison of both sensors after the experiment.

Experimental Procedure

The experiment was split up into three one-hour-sessions on consecutive days. The experiment was conducted by one of two experimenters, who knew about the hypotheses and also took part in the study as subjects (subject number 1 and 6). At the beginning of each session, room and VE orientation were aligned manually. During this procedure, subjects positioned themselves in the middle of the laboratory and put on the backpack and the HMD. The experimenter could then rotate the VE by 180° with a button press. Since the PPT had two indiscernible LEDs that were fixed to the HMD to track the orientation, two initialization angles were possible. If the subject pointed at a transparent pillar 3 m in front of the starting position in the VE, while pointing at a specific point in the lab, the first alignment was completed. From then on, the gyro-sensors of the HMD were used to detect any head rotations during the experiment.

At the beginning of the first session all subjects were given a participant information form and were asked to sign a declaration of consent. Afterwards, they got a detailed instruction by the experimenter (see Appendix 1 for the complete manuscript) and were motivated to ask comprehension questions. Before and after every session, the simulator sickness questionnaire (SSQ) was filled out to measure motion sickness (Kennedy, Lane, Berbaum, & Lilienthal, 1993). Additionally, the Slater-Usuh-Steed questionnaire for immersion (SUS) was answered at the end of each session (Usuh, Catena, Arman, &

Slater, 2000). All sessions consisted of four different tasks that are described below. An Overview of all three sessions can be found in Figure 2. Participants were allowed to take breaks at any time.

Straight Walking & Pointing Task. In this part of the experiment, subjects had to go to a transparent pillar to start a trial. A red bullseye-target with a radius of 1.5 m and a height of 0.7 m appeared at the other end of the laboratory in a distance of 8 m. Then, the subject had to orient towards the target for it to turn blue. After pointing at the target and pressing a button on the controller, the tracking system obtained the pointing direction and a reloading sound was played. If the subject was still looking towards the target, it turned green. Then, the subject had to pull a trigger on the controller to shoot at the target with an invisible gun. A shooting sound was played and the target disappeared. Next, the subject had to walk in the direction of the target. After 5.75 m, an arrow appeared indicating to turn around and go back to the transparent pillar. Each straight walking & pointing block consisted of five trials.

Threshold Measurement. To measure the perceptual threshold for curvature gains, we tested seven different gains with nine trials per gain (see Table 1 for transformation in radius) in an equal pseudorandom order that was also equal in each threshold block for every subject. In each trial, the subject had to walk on a white path flanked by two transparent pillars at each side of the VE (see Figure 2), while a curvature gain of $\frac{\pi}{30}$ was applied. When the subject had reached the destination pillar a head fixed decision menu appeared (see Figure 4).

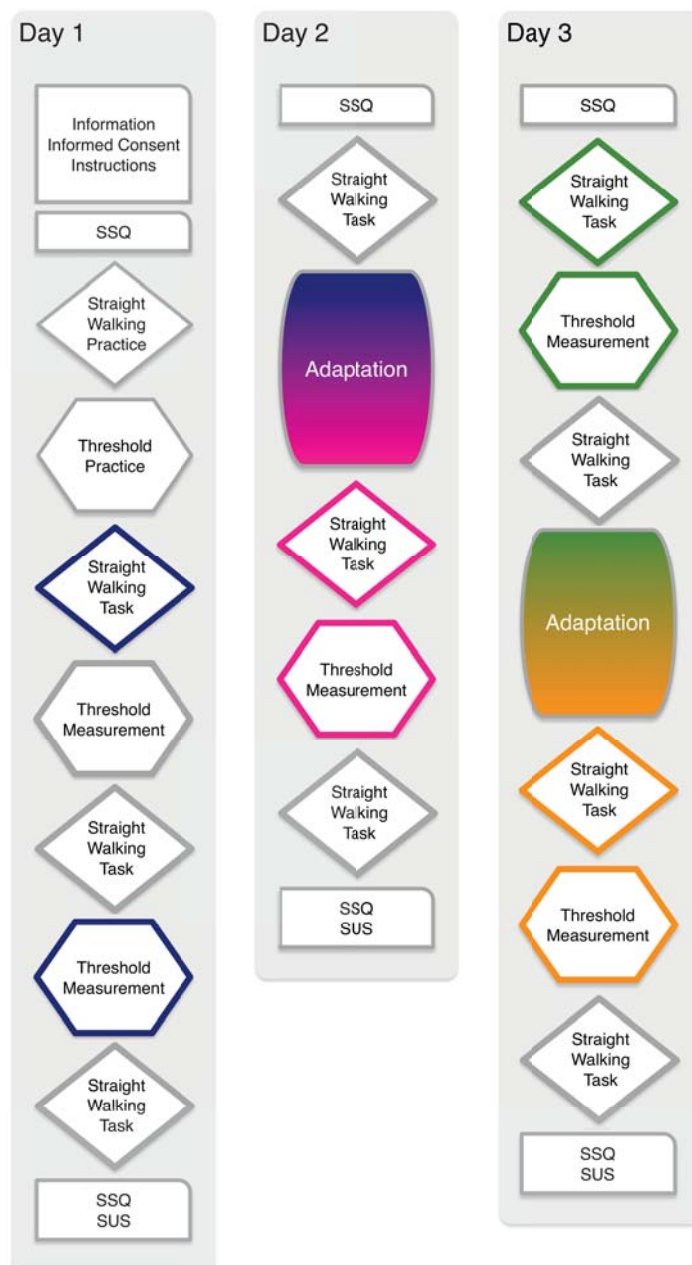


Figure 2. Overview of the experimental procedure. The experiment was split up into 3 one-hour-sessions. On day 1 the tasks were practised and Baseline measurements were done (blue). On the next day, the same measurements were taken after the First Adaptation of 150 adaptation trials (magenta). Day 3 started with measurements for Carry-Over-effects (green). Afterwards, a Second Adaptation block, the straight walking task and the threshold measurement were completed (orange).

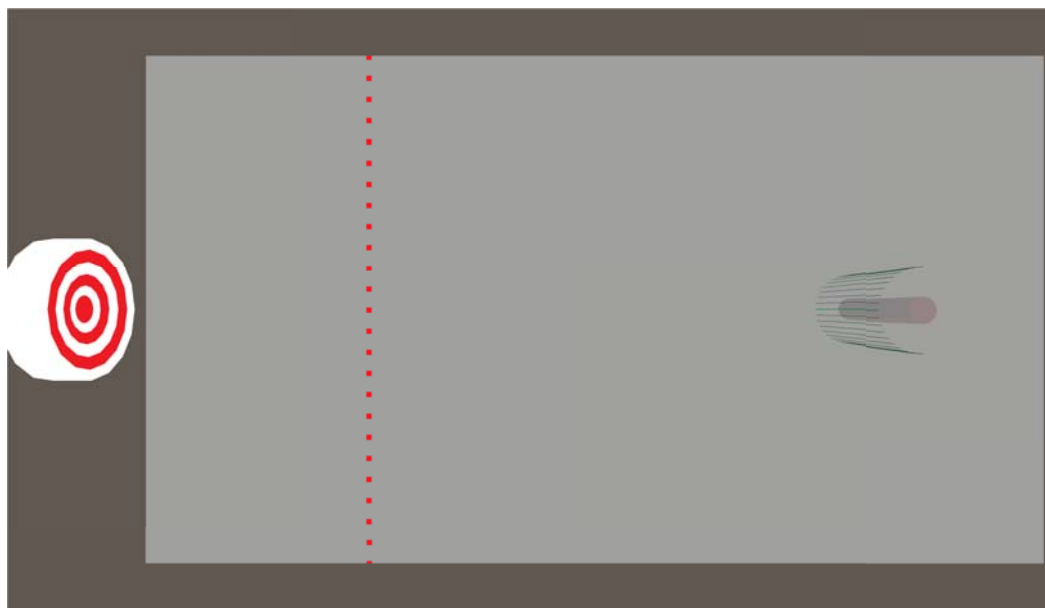


Figure 3. Top view of the Straight Walking & Pointing Task. If the subject walked into the transparent pillar on the right, the trial was started and the target appeared. The pointing direction of the controller was calculated using the center of the pillar and the position of one of 180 invisible pillars (shown in green) that were placed around the subject with a radius of 40 cm. When the tracked controller was colliding with one of them, a new pointing vector was calculated. After subjects shot the target with an invisible weapon, the target disappeared and they walked without visual feedback until they crossed the invisible line (shown in red) at 5.75 m.

At the end of each threshold trial, subjects were able to see a score between 0 and 100, indicating how accurately they were walking on the given path in the last trial. The score was calculated by dividing the mean distance to the origin of the curvature gain circle during the trial by the radius defining the applied curvature gain. The points were given in a linear decreasing distribution with 100 points at a mean deviation of zero and a cut-off value at a mean deviation of 0.5 m.

Table 1. Curvature Gains and Radii.

gC (m^{-1})	$-\pi/15$	$-\pi/30$	$-\pi/60$	0	$+\pi/60$	$+\pi/30$	$+\pi/15$
radius (m)	-4.77	-9.55	19.1	∞	19.1	9.55	4.77

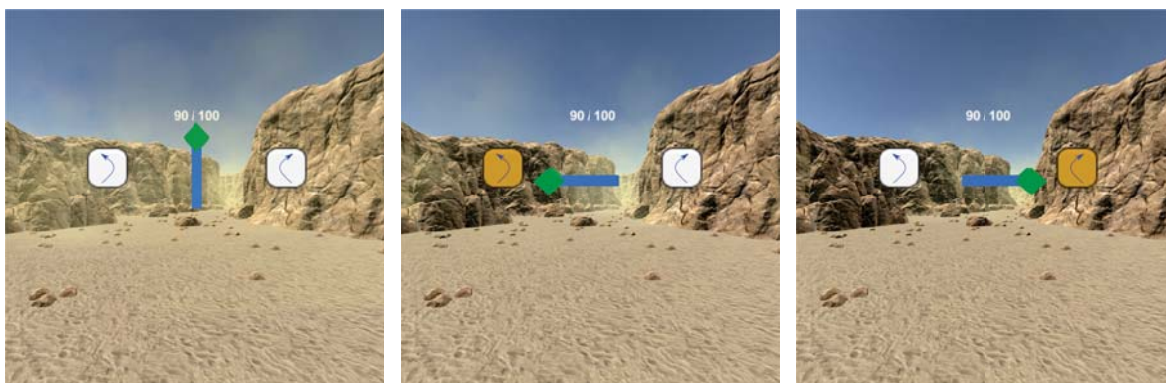


Figure 4. Decision menu for 2AFC-like task. After subjects did one trial with an unknown gain, they had to decide whether they were redirected to the right or to the left, by pressing the according button on the controller. Decisions could be corrected or confirmed by pressing a second button. Points were shown only during the threshold measurement phase.

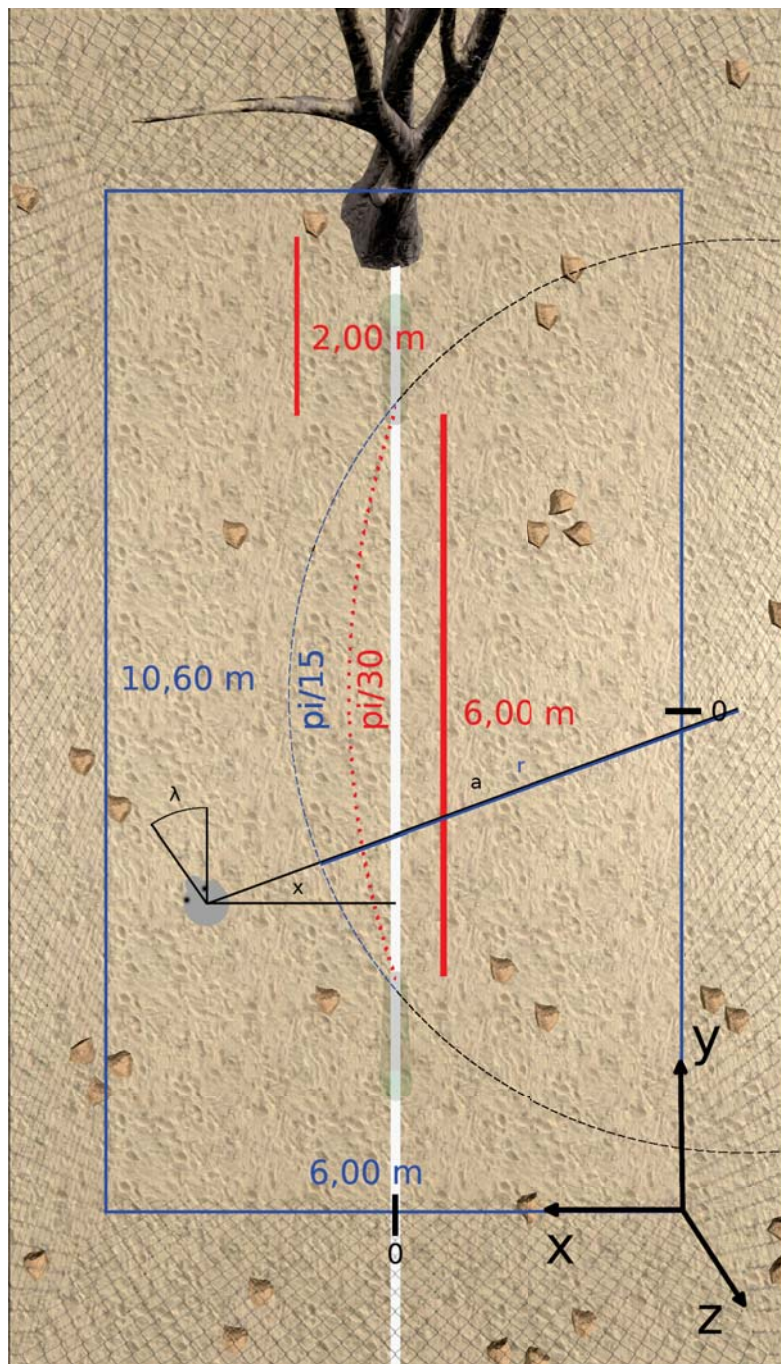


Figure 5. The VE for threshold, instructional and adaptational blocks from above. The position of the subject is shown in grey. Blue box: tracked space, dotted coloured lines: ideal physical path according to different curvature gains, the tree swapped positions according to the starting position. λ = real orientation, r = radius of the curvature gain circle, a = distance between the origin of the circle and the subject.

Then subjects could decide whether they perceived walking on a leftward or a rightward curve during the last trial with a button press on the controller, while the menu changed according to their input (see Figure 4). Hereafter they could alter their input or confirm it. After the confirmation, a sound was played and the VE was masked with a grey screen for 0.5 seconds and the subject had to turn around. When the pillar was left, the next trial started. To prevent any mistakes after the masking, a tree was placed behind the starting pillar in the VE, so subjects would not walk into the wrong direction, when starting the next trial.

Instructional Block. To resolve possible instructional misunderstandings, this block was done at the beginning of the first session. It consisted of a shortened threshold block with seven different gains. After the seventh trial, a pillar appeared and the subject could walk into it to continue with the next block. Subjects were able to do more testing trials with a random gain from the threshold measurement set if they wanted.

Adaptation. During the adaptation block, the subject had to walk on a white path between two transparent pillars at each side of the VE (see Figure 5) for 150 trials. During this procedure, a constant curvature gain of $\frac{\pi}{30}$ was applied. When the subject reached the destination pillar a sound was played, the VE was masked for 0.5 seconds and the subject had to turn around. When the pillar was left, the next trial started. To prevent any mistakes after the masking, a tree was placed behind the starting pillar in the VE, so subjects would not walk into the wrong direction, when starting the next trial.

Curvature Gain

To make sure that the start and ending positions of the subjects were fix for every trial, we used a constant curvature gain algorithm. The yaw rotation angle of the VE α ,

changed according to the applied gain with a radius r , the yaw rotation of the subjects HMD λ and the distance between the subject and the origin of the circle defining the curvature gain a .

$$\alpha = \lambda + \frac{180}{\pi} * \text{Acos}\left(\frac{x^2 - r^2 - a^2}{-2|r|a}\right)$$

This led to ideal walking paths of different lengths (see Figure 5). An example of simulated α -values can be found in Appendix 2.

Statistical Tests

Statistical tests and plots were done with R version 3.4.2 (R Core Team, 2013). Additionally, perceptual threshold curves were fitted and plotted using Matlab R2018b (MATLAB, 2018).

To check if the gathered data fulfilled the requirements of linear testing, QQ-plots, Shapiro-Wilk tests (Shapiro & Wilk, 1965) and histograms were regarded. If a normal distribution could be assumed, random effect models and post-hoc tests were calculated using the lme4 (Bates, Mächler, Bolker, & Walker, 2015) and lmerTest (Kuznetsova, Brockhoff, & Christensen, 2017) packages in R. In other cases, Friedman tests (Friedman, 1937) and post-hoc pairwise Wilcoxon rank-sum-tests (Wilcoxon, 1945) were used. Hedges' g (Hedges & Olkin, 1985) was calculated for differences with $p < .05$.

For the threshold measurements, logistic psychometric curves of the form

$$S(x; m; w) = \frac{1}{1 + e^{-2 \log\left(\frac{1}{0.05} - 1\right) \frac{x-m}{w}}}$$

were fitted to the threshold answers of each condition for all subjects using the psignifit4 package (Schütt, Harmeling, Macke, & Wichmann, 2016) for Matlab. In this function, S is a strictly monotonic, scaled sigmoid function of the stimulus level x that ranges from 0 for low levels to 1 for high levels, m provides the mean and w provides the width.

The resulting parameters including the point of subjective equality (PSE), perceptual thresholds and slopes, were then analysed as explained above.

Results

First, the tracking data of the position tracking system is described. Afterwards, an overview of the results of the pointing task is given and the answers of the threshold blocks of all subjects are used to calculate and analyse perceptual thresholds. Lastly, the results of the orientation sensors and the questionnaires that were answered during the experiment are outlined.

Tracking Data

The base of all statistical analysis of the tracking data was the mean of the calculated positions from the two tracked LEDs that were corrected for their position on the HMD and then filtered using a Kalman filter (1960).

Pointing Task. Pointing directions were measured for each Walking Trial for each subject by identifying the last invisible pillar that was hit with the controller during the pointing task. Since the objects were placed in a semicircle around the starting point, each of them represented one pointing direction from -90 (left) to 90 (right) in steps of one degree. The mean direction over all trials and subjects was -10.43° ($SD = 24.44$). Figure 6 shows that a pointing error to the left side can be seen in all conditions. A Shapiro-Wilk test indicated that the sample was significantly different from a sample of normal distributed data ($W = 0.95$, $p < .001$). A Friedman test did not show a significant difference between the Baseline condition and the pointing tasks after adaptation and the Carry-Over condition ($\chi^2 = 3.7$, $p > .05$).

Straight Walking Task. The average position in x-direction of all positions at the minimum and the maximum position in y-direction during the Straight Walking Task were calculated for every trial. The lateral movement (in x-direction) of each trial was then calculated by the distance of both values. The QQ-plot and the histogram of

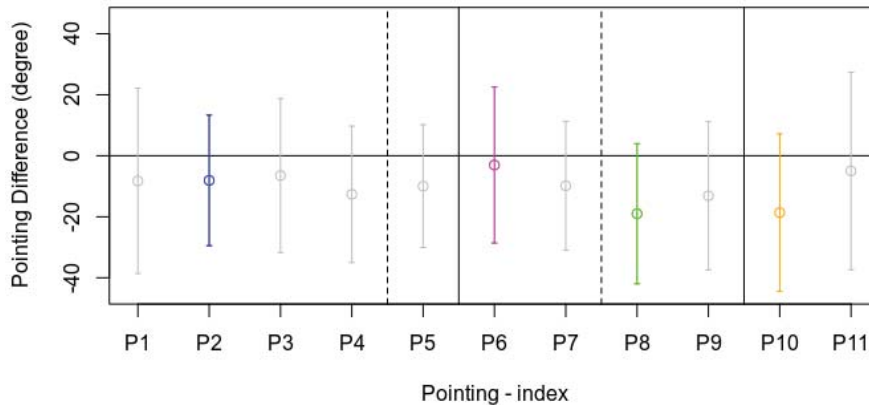


Figure 6. Means of pointing directions during the Pointing Task. Directions were averaged over trials and subjects. Dotted lines indicate the next session, continuous lines show adaptation blocks. P2 (blue) was used as Baseline, P6 (magenta) and P10 (orange) were used to see possible effects of adaption. P8 (green) was measured to check for Carry-Over-effects. Error bars show 1 standard deviation.

the data indicated a normal distribution and a Shapiro-Wilk test showed no significant difference ($W = 0.99$, $p > 0.05$). Figures 7 and 8 show that in both Straight Walking Tasks after adaptation, subjects did lateral movements to the right.

To test this effect, a linear model of the lateral movement of every trial was fitted. A model including the factor Subject outperformed a fixed effect model without this factor ($F = 10.11$, $p < .0001$). Since we were not interested in differences between single subjects, a random effects model with Subject as random factor was fitted. Adding Trial as a factor to the model did not lead to significant improvement ($\chi^2 = 2.16$, $p > .05$) and was therefore, not included. The residual plot of the resulting model can be seen in Appendix 3. All estimates can be interpreted as mean differences between the Baseline and the respective condition. The intercept did not show a significant difference from

zero, indicating that subjects did walk in a straight line in the Baseline condition ($W2: Baseline = .00, p > .05$). The model demonstrated a significant difference between the Baseline and both conditions after adaptation ($W6: First\ Adaptation = .19, g = 0.34, p < .05$; $W10: Second\ Adaptation = .52, g = 1.26, p < .0001$), but not for the condition on day three ($W8: Carry-Over = .07, p > .05$). The random effect Subject could explain 31.3% of the variance.

Post-hoc t-tests showed significant differences between both Straight Walking Tasks on day 3 W8 and W10 ($g = 0.7, p < .0001$) and between the two conditions after adaptation W6 and W10 ($g = 0.6, p < .001$). An overview of all posthoc comparisons can be seen in Figure 9.

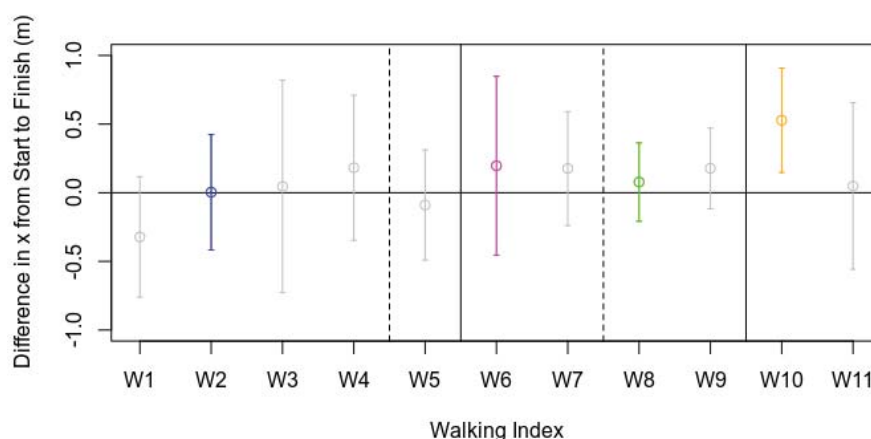


Figure 7. Means of lateral movements during the straight walking task. Lateral movements were averaged over trials and subjects. Dotted lines indicate the next session, continuous lines show adaptation blocks. W2 (blue) was used as Baseline, W6 (magenta) and W10 (orange) were used to see possible effects of adaption. W8 (green) was measured to check for Carry-Over-effects. Error bars show 1 standard deviation.

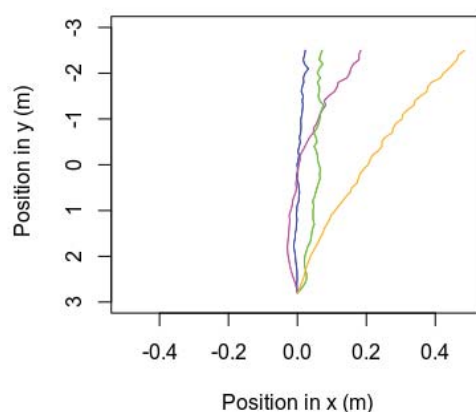


Figure 8. Paths of the Straight Walking Task. All positions in x of the 5 trials of each walking block were averaged per rounded y positions, trials, subjects and condition. All paths were then corrected for their starting position. Because there were still big variances, a sliding mean with a width of 0.5 m was applied to the 4 walking paths. A mapped version of the paths can be found in Appendix 3.

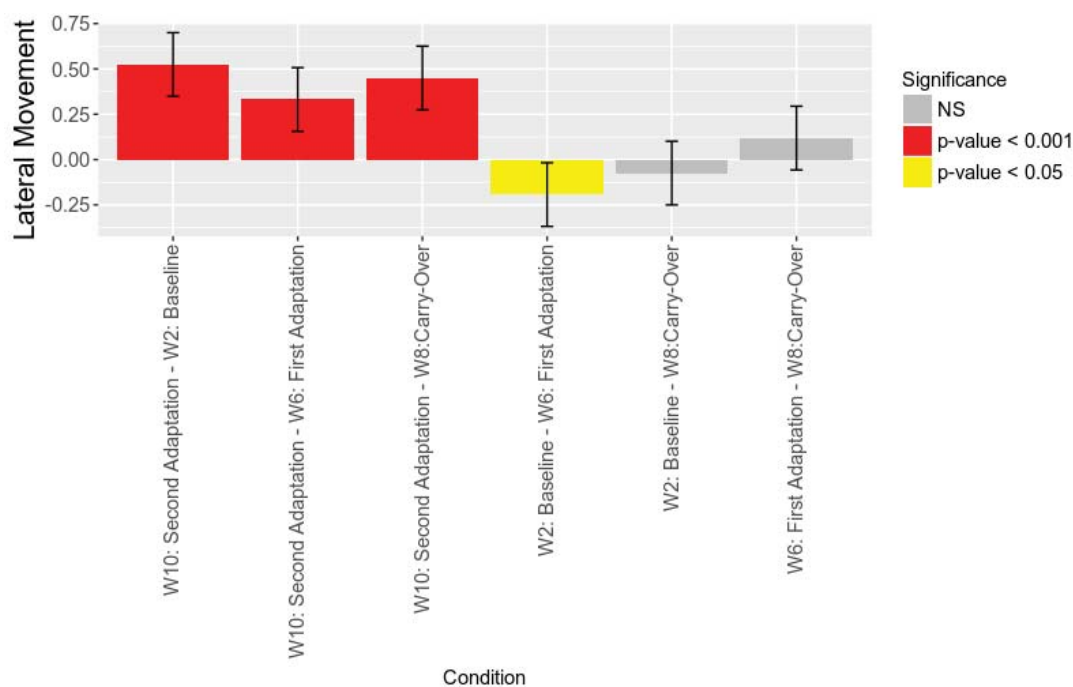


Figure 9. Results of the Straight Walking Task. Corrected post-hoc comparisons of the lateral movements of the different conditions from the random effect model. Error bars show two-sided 95% confidence intervals.

Adaptation. The first adaptation block took in average 25.37 minutes ($SD = 9.06$), while the second adaptation block took 20.98 minutes ($SD = 5.48$). Due to technical issues, tracking data was not saved for the second adaptation session of subject 5. If subjects would have followed their path perfectly, they would have travelled a minimum tracked distance of 915.5 m. In the first adaptation session, a mean distance of 1067.85 m ($SD = 72.69$ m) was walked, while subjects travelled 1020.59 m ($SD = 42.93$ m) in the second block. Figure 10 shows the position pattern of a typical subject for a complete adaptation block.

Threshold Measurement. All threshold blocks took in average 11.49 minutes ($SD = 2.19$). The mean distance the subjects travelled was 457.55 m ($SD = 22.48$ m). Figure 11 shows the position pattern of a typical subject for one complete threshold block. A Shapiro-Wilk test ($W = 0.98, p > .05$), the QQ-plot and the histogram (see Appendix 4) indicated that all assumptions for linear modeling of the data were fulfilled. The resulting average speeds were predicted using a random effects model with Subject as random effect ($F = 7.03, p < .05$) and Condition as fixed effect. The conditions did not differ significantly from the Baseline ($Baseline = 0.67$ m/s ($SD = 0.09$), $First\ Adaptation = 0.64$ m/s ($SD = 0.08$), $Carry-Over = 0.73$ m/s ($SD = 0.11$), $Second\ Adaptation = 0.71$ m/s ($SD = 0.14$), all $p > .05$). The random effect Subject explained 35.2% of the variance. The residual plot of the model can be seen in Appendix 4.

Post-hoc tests revealed that the speed in First Adaptation and Carry-Over were significantly different from each other ($Difference = 0.08$ m/s, $g = 0.81, p < .05$).

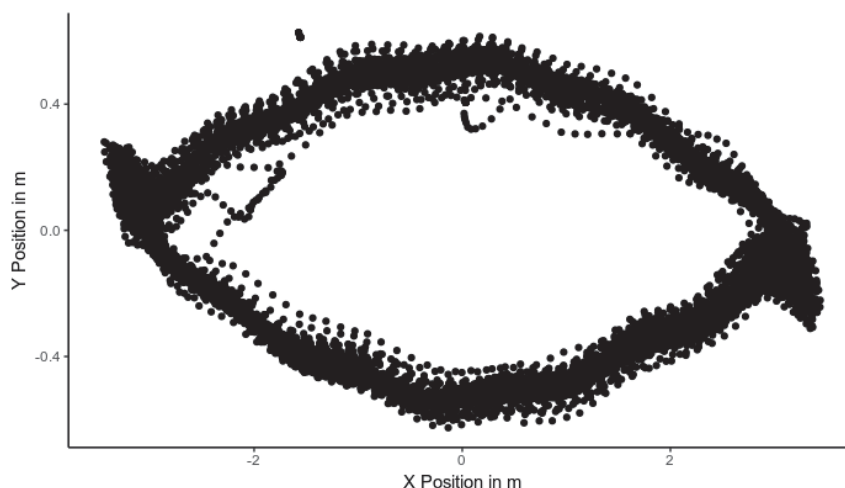


Figure 10. Typical tracking data of an adaptation block of one subject. During the adaptation, a constant curvature gain of $\frac{\pi}{30}$ was applied. Subjects were instructed to walk on a white straight path in the VE and to turn around every time they reached a transparent pillar.

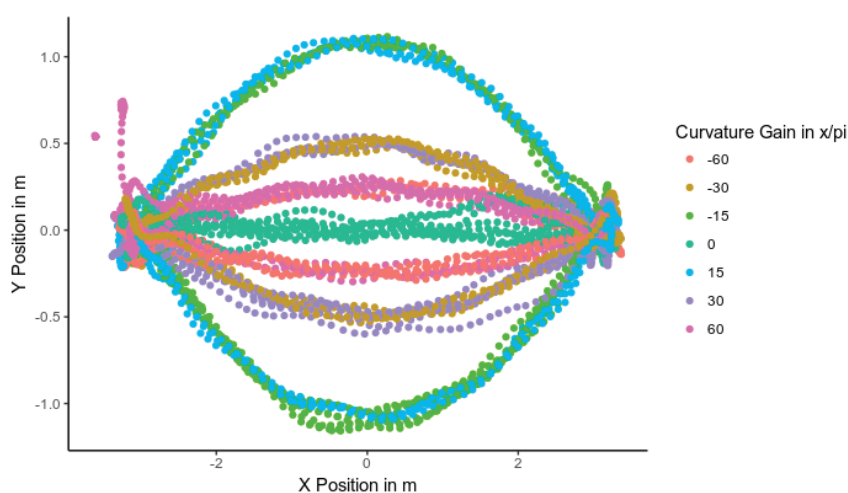


Figure 11. Typical tracking data of a threshold block of a subject. The pattern of the 7 different curvature gains that were applied can clearly be seen. Subjects were instructed to walk on a white straight path in the VE and choose the direction in which they were redirected after each trial. Leftward and rightward gains were applied at both starting points in a pseudorandom order.

Perceptual Thresholds

With the answers subjects gave during the 2AFC-like task during the threshold measurements, logistic psychometric curves were fitted. Two subjects (3 and 12) had to be excluded from the analysis because applying the defined curves to their data resulted in no reasonable fit. The raw data and the fitted curves of all subjects can be found in Appendix 4. The different parameters of the fitted curves were then tested separately. In Figure 12, the psychometric curves were fitted over all subjects for each condition, to visualize the perceptual thresholds.

PSE: The point of subjective equality is the gain at which participants perceive their physical path as straight or normal and for which they cannot decide whether the curvature was leftward or rightward. In this case, they have to guess the direction of curvature and report rightward and leftward gains each with a probability of 50%. Differences of PSE values in the different conditions were tested in m^{-1} to achieve normally distributed data and define small curvature gains as close to 0. A Shapiro-Wilk test revealed that PSEs did not differ significantly from a sample of a normal distribution ($W = 0.97$, $p > 0.05$). The histogram and the QQ-plot of the data can be seen in Appendix 4.

To test if the conditions led to significantly differing PSEs, a linear model using Condition to predict the PSE was fitted. A model including the factor Subject outperformed a fixed effect model without this factor ($F = 10.04$, $p < .0001$). Since we were not interested in differences between single subjects, a random effects model with Subject as random factor was fitted. The residual plot of the resulting model can be seen in Appendix 4.

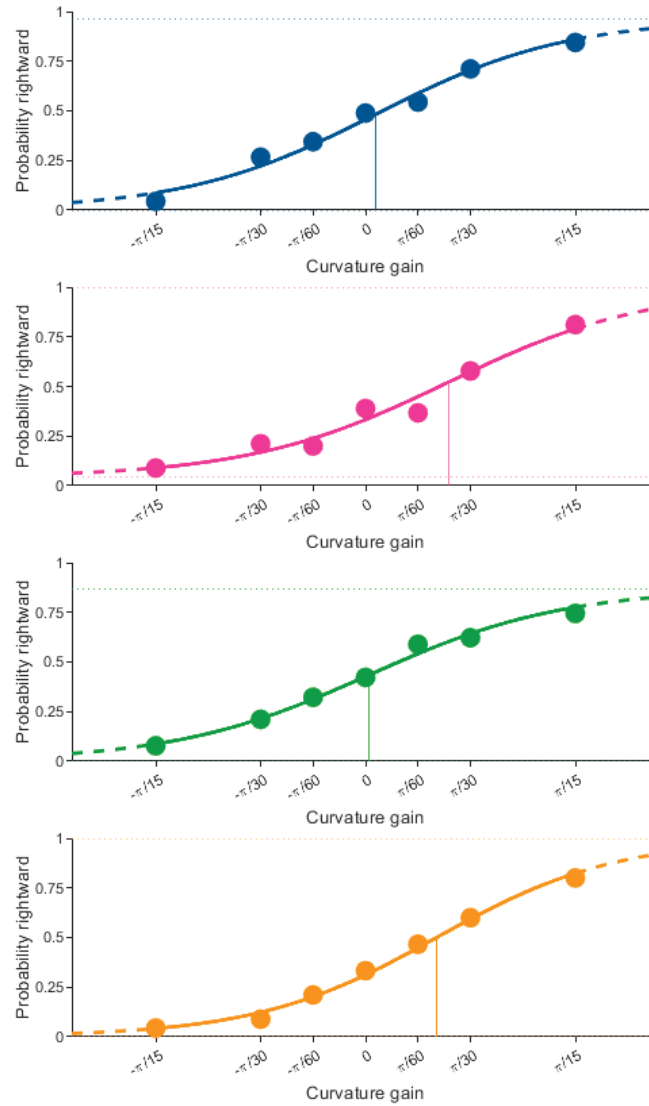


Figure 12. Logistic psychometric curves of the form $S(x; m; w) = \frac{1}{1 + e^{-2 \log\left(\frac{1}{0.05} - 1\right) \frac{x-m}{w}}}$ that were fitted to the threshold answers of each condition over all subjects using the psignifit4 package (resulting radii: Baseline (blue): PSE: 97.29 m, 25%-Threshold: 11.14 m, 75%-Threshold: 7.75 m, First adaptation (magenta): PSE: 12.1 m, 25%-Threshold: 22.24 m, 75%-Threshold: 5.36 m, Carry-Over (green): PSE: 273.3 m, 25%-Threshold: 11.82 m, 75%-Threshold: 5.48 m, Second adaptation (orange): PSE: 14.08 m, 25%-Threshold: 36.17 m, 75%-Threshold: 14.08 m).

The intercept can be interpreted as mean of the Baseline and was not significantly different from 0 ($Intercept = -0.006, p > .05$). All estimates in the final model can be interpreted as mean differences. The PSEs of all conditions were significantly different from the Baseline ($First\ Adapt = 0.08, p < .0001$; $Carry-Over = 0.022, p < .001$; $Second\ Adapt = 0.066, p < .0001$). The random effect Subject could explain 69.3% of the variance. Post-hoc t-tests revealed that all conditions were significantly different from each other. An overview can be seen in Figure 13.

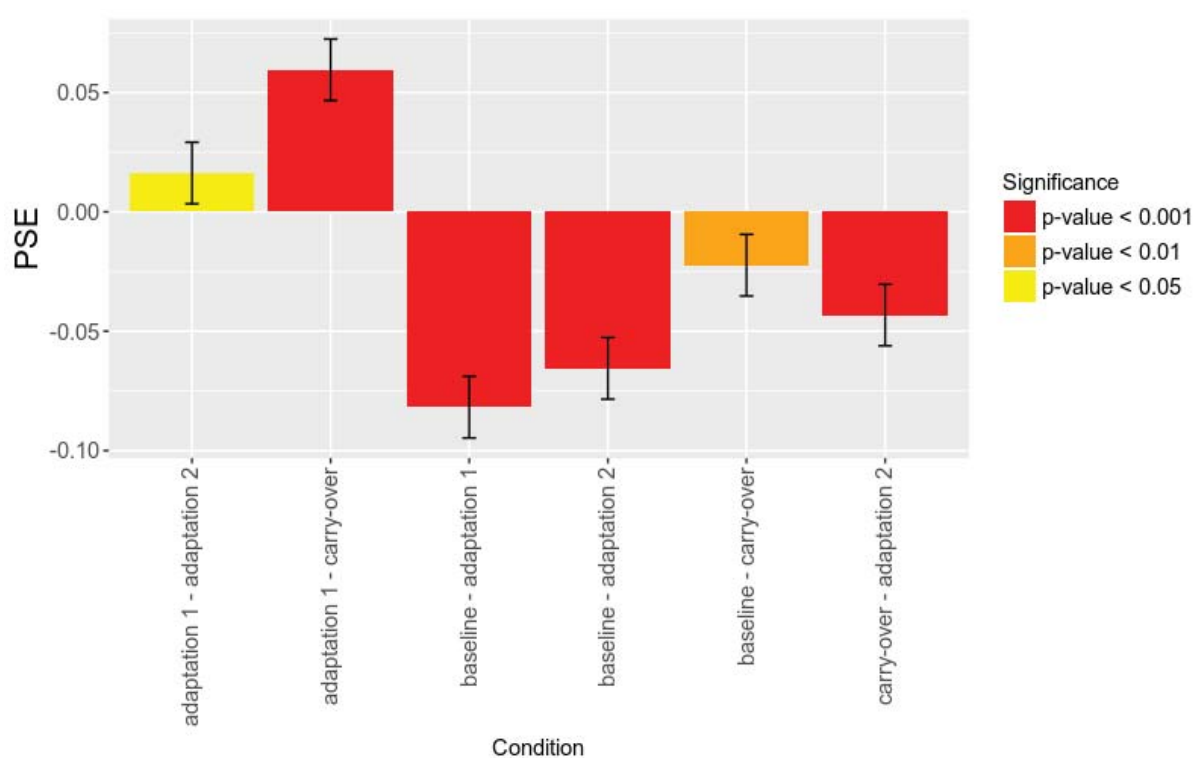


Figure 13. Mean differences of the PSEs of all threshold measurements that resulted from post-hoc t-tests. Error bars show two-sided 95% confidence intervals.

75%-Threshold: The 75%-Threshold is the gain at which participants perceive being redirected rightwards. In this case, they do not have to guess the direction of curvature and report being redirected rightwards with a probability of 75%. Differ-

ences of the threshold values in the different conditions were tested in m^{-1} to achieve normally distributed data and define small curvature gains as close to 0. A Shapiro-Wilk test revealed that the distribution of thresholds did differ significantly from a sample of a normal distribution ($W = 0.88$, $p < 0.001$). This effect was mainly driven by the thresholds of subject 1, so they were excluded. But even including them did change the results only marginally (see below). A second Shapiro-Wilk test without subject 1 was not significant ($W = 0.96$, $p > 0.05$). The histogram and the QQ-plot of the original data can be seen in Appendix 4. To test if the conditions led to significantly differing thresholds, a linear model using Condition to predict the 75%-Threshold was fitted. A model including the factor Subject outperformed a fixed effect model without this factor ($F = 26.45$, $p < .0001$). Since we were not interested in differences between single subjects, a random effects model with Subject as random factor was fitted. The residual plot of the resulting model can be seen in Appendix 4.

The intercept can be interpreted as mean of the Baseline and was significantly different from 0 ($Intercept = 0.11$, $p < .0001$). All estimates in the final model can be interpreted as mean differences from the Baseline. The 75%-Thresholds of all conditions were significantly different from the Baseline ($First Adapt = 0.04$, $p < .0001$; $Carry-Over = 0.02$, $p < .0001$; $Second Adapt = 0.03$, $p < .0001$). The random effect Subject could explain 86.4% of the variance. Post-hoc t-tests revealed that except for Baseline and Carry-Over, all conditions were significantly different from each other. When the thresholds of subject 1 were included in the analysis, there was no significant difference between Carry-Over and Second Adaptation. A comparison of all post-hoc t-tests can be seen in Figure 14.

25%-Threshold: The 25%-Threshold is the gain at which participants perceive being redirected leftwards. In this case, they do not have to guess the direction of curvature and report being redirected rightwards with a probability of only 25%. Differences of the threshold values in the different conditions were tested in m^{-1} to achieve normally distributed data and define small curvature gains as close to 0. A Shapiro-Wilk test revealed that the distribution of thresholds did not differ significantly from a sample of a normal distribution ($W = 0.95, p > 0.05$). The histogram and the QQ-plot of the data can be seen in Appendix 4.

To test if the conditions led to significantly differing 25%-thresholds, a linear model using Condition to predict the threshold was fitted. A model including the factor Subject outperformed a fixed effect model without this factor ($F = 5.7, p < .001$). Since we were not interested in differences between single subjects, a random effects model with Subject as random factor was fitted. The residual plot of the resulting model can be seen in Appendix 4.

The intercept can be interpreted as mean of the Baseline and was significantly different from 0 ($Intercept = -0.1, p < .0001$). All estimates in the final model can be interpreted as mean differences from the Baseline. All conditions were significantly different from the Baseline ($First Adapt = 0.081, p < .00001$; $Carry-Over = 0.03, p < .00001$; $Second Adapt = 0.078, p < .00001$). The random effect subject could explain 54% of the variance. Post-hoc t-tests revealed that all conditions were significantly different from each other except for the two adaptation conditions. A comparison of all post-hoc t-tests can be seen in Figure 15.

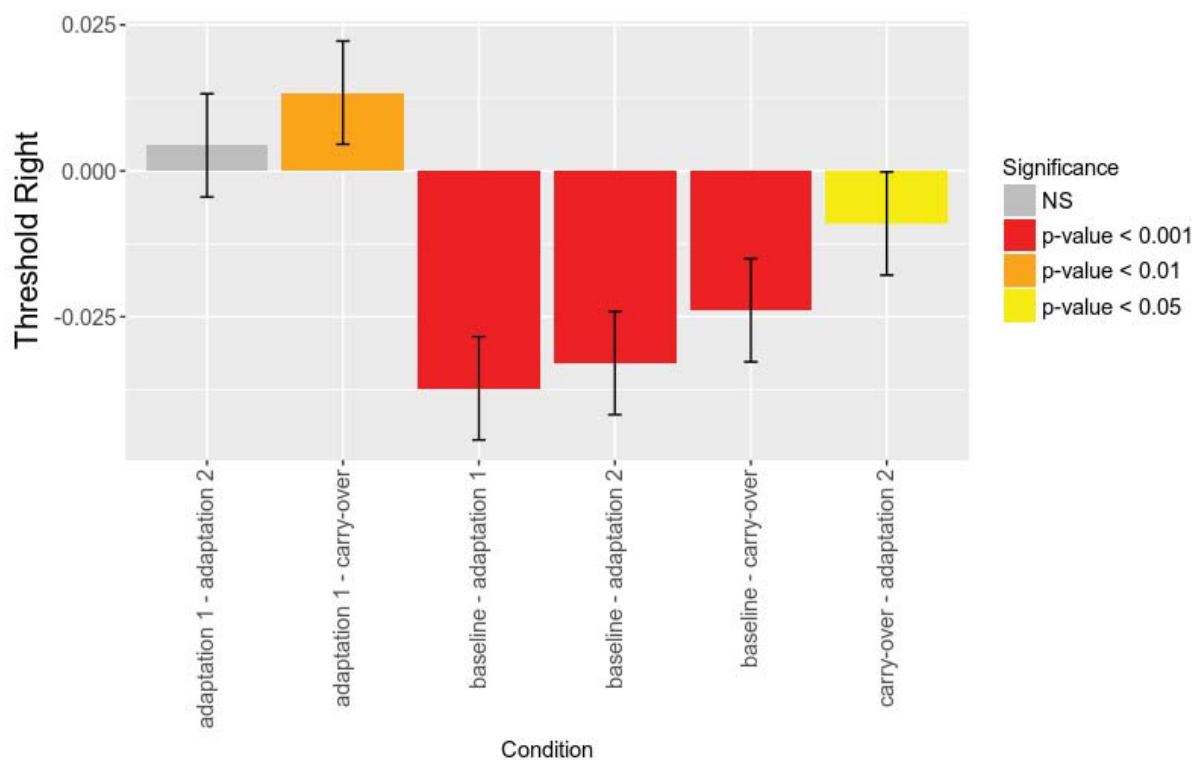


Figure 14. Mean differences of the 75%-Thresholds of all measurements that resulted from post-hoc t-tests. Error bars show two-sided 95% confidence intervals.

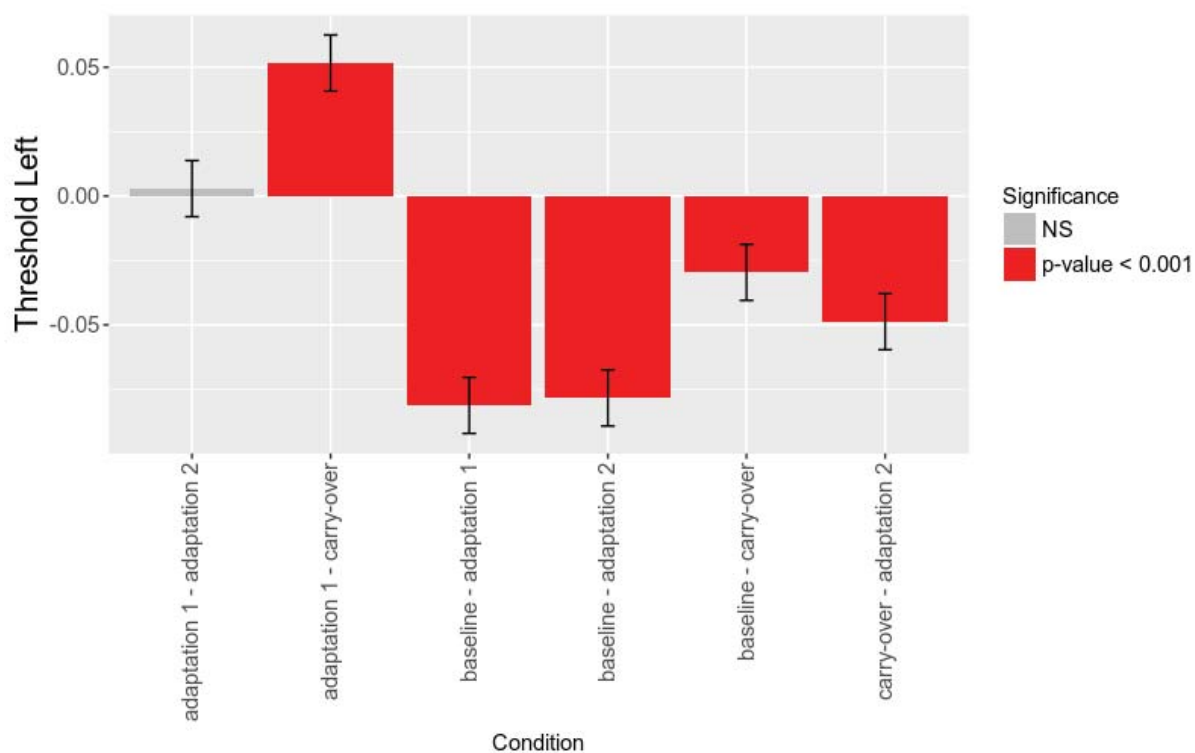


Figure 15. Mean differences of the 25%-Thresholds of all measurements that resulted from post-hoc t-tests. Error bars show two-sided 95% confidence intervals.

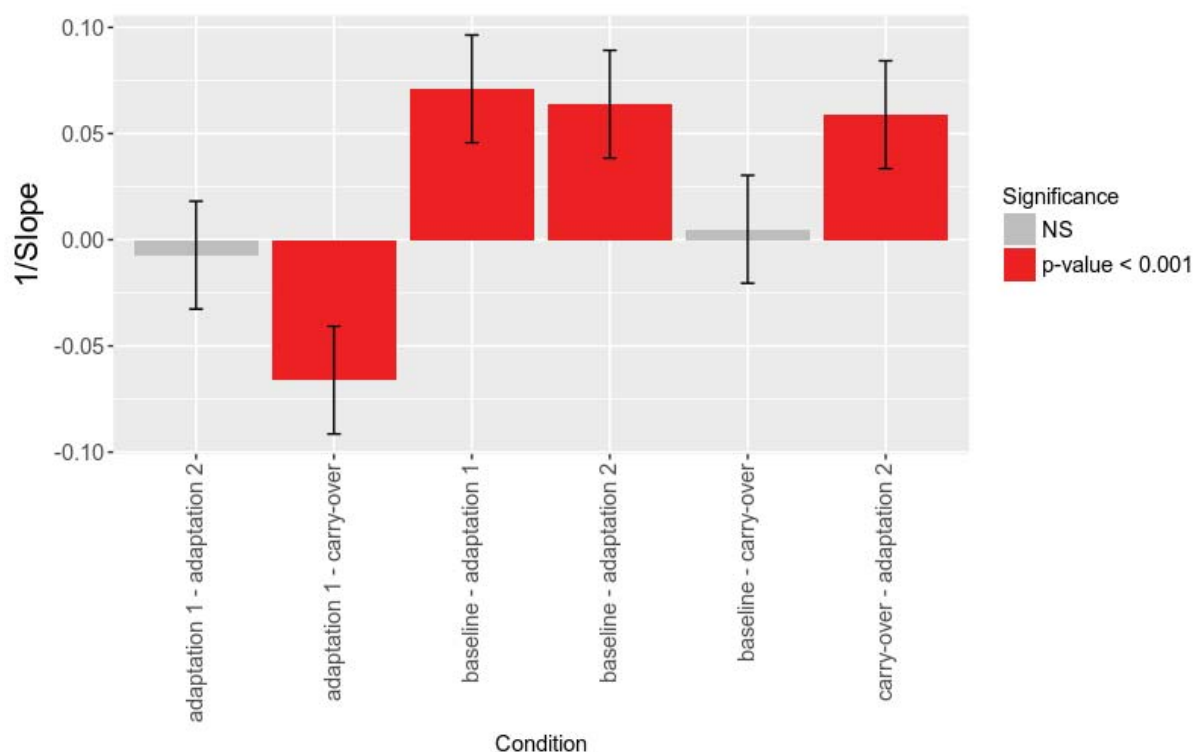


Figure 16. Mean differences of the inverse Slopes of all conditions that resulted from post-hoc t-tests. Error bars show two-sided 95% confidence intervals.

Slope: The Slope at the PSE indicates how wide the perceptual thresholds spread, while low values indicate flat psychometric curves. Differences of the slopes in the different conditions were tested as their inverse to achieve normally distributed data. A histogram of the original left skewed data can be found in Appendix 4. A Shapiro-Wilk test revealed that the distribution of transformed slopes did not differ significantly from a sample of a normal distribution ($W = 0.96$, $p > 0.05$). The histogram and the QQ-plot of the transformed data can be seen in Appendix 4.

To test if the conditions led to significantly differing slopes, a linear model using condition to predict the inverse slope was fitted. A model including the factor Subject outperformed a fixed effect model without this factor ($F = 19.22$, $p < .0001$). Since we were not interested in differences between single subjects, a random

effects model with Subject as random factor was fitted. The residual plot of the resulting model can be seen in Appendix 4.

The intercept can be interpreted as the inverse mean slope of the Baseline and was significantly different from 0 (*Intercept* = 0.356, $p < .0001$). All estimates in the final model can be interpreted as inverse mean slope differences from the Baseline condition. The slopes of the adaptation conditions were significantly steeper than the slope from the Baseline (*First Adapt* = -0.071, $p < .0001$; *Second Adapt* = -0.064, $p < .0001$). The random effect subject could explain 82% of the variance. Post-hoc t-tests revealed that the two adaptation conditions were significantly different from the Carry-Over condition ($p < .0001$). A comparison of all post-hoc t-tests can be seen in Figure 16.

An overview of the mean values of all parameters of the four conditions and the effect-sizes can be found in Appendix 4.

Orientation Tracking

During all experimental sessions, the orientation of the HMD was realigned with the position tracking system after every trial. Since the orientation sensor of the HMD seemed to show a systematic drift, the correction angle that was applied on the original data varied over time and between subjects (*Median^{slope}* = -0.35° per minute (range from -2.86 to 3.63)). Figure 17 shows a typical set of orientation data from both devices and the correction value over time.

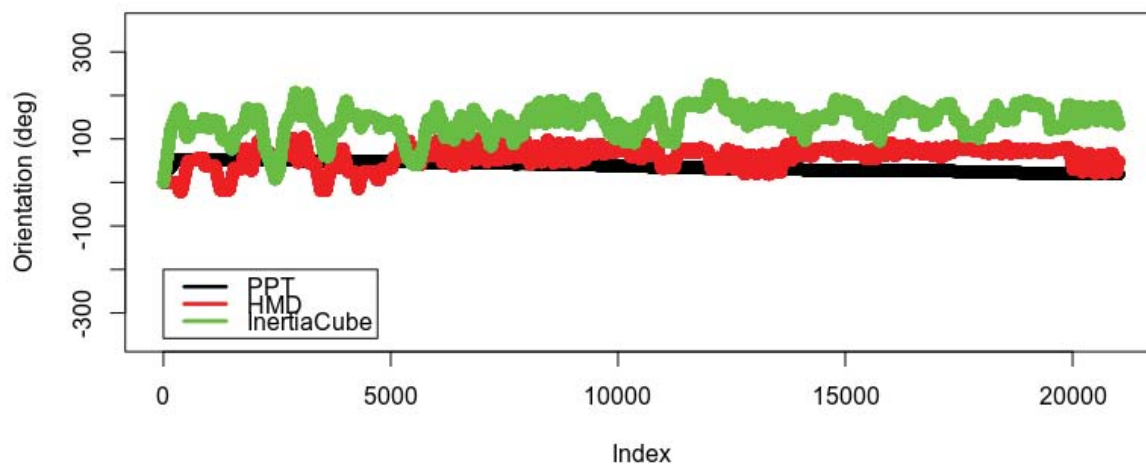


Figure 17. To compare the orientation data of the InertiaCube 3 and the HMD, the data of both devices was filtered using a sliding mean with a bandwidth of 375 data points which is equal to a time window of approximately 60 seconds. All values were corrected for their starting value.

Questionnaires

On each day, participants completed the SSQ before and after their session. Subjects could classify the emerging of 16 symptoms of motion sickness in the categories None, Slight, Moderate and Severe. A total value was calculated using the weighted mean according to the manual, resulting in higher values for stronger motion sickness (Kennedy et al., 1993). The mean post-pre difference in SSQ score was largest on the first day (13.3, ($SD = 17.2$)) and lower on the following days (day 2: 4.9, ($SD = 6.8$), day 3: 7.8 ($SD = 4.9$)).

For the SUS, subjects described their sense of being in the virtual environment, on a scale from one to seven, where seven represents the most realistic experience, in six items (Usuh et al., 2000). The mean SUS score was 4.1 ($SD = 1.8$) and did not change

over the course of adaptation (day 1: 4.3, ($SD = 1.7$), day 2: 4.0, ($SD = 1.8$), day 3: 4.0, ($SD = 1.8$)). The results from both questionnaires can be found in Figure 18.

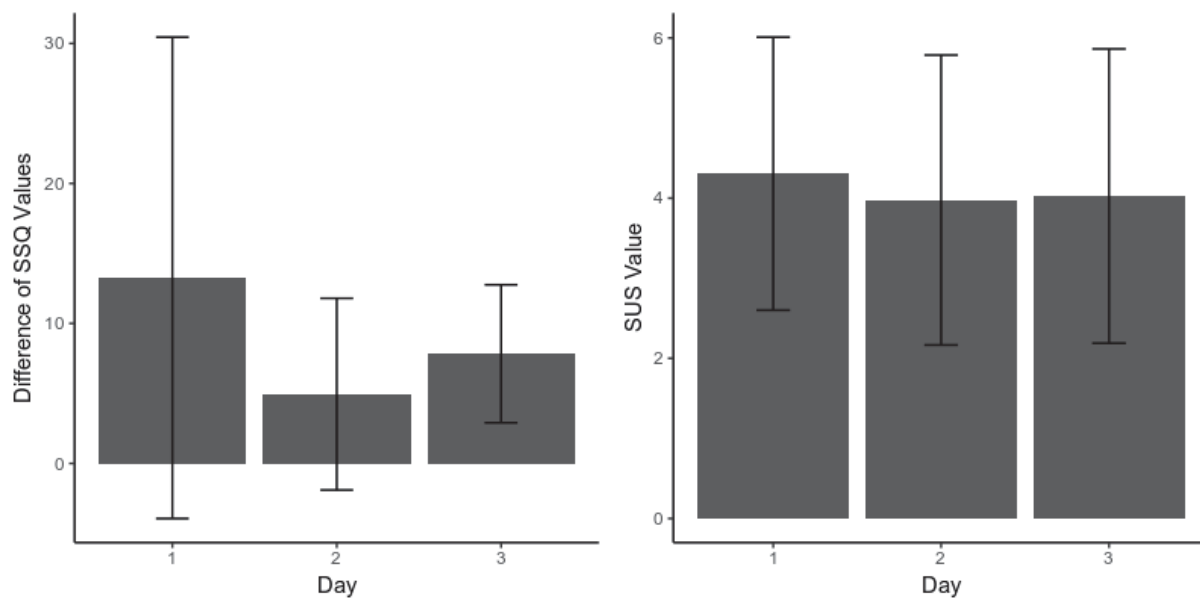


Figure 18. Results from the questionnaires. Left: The differences between post- and pre-SSQ values were calculated for each subject individually and then averaged over all sessions. Right: SUS values were averaged over all subjects. Error bars show 1 standard deviation in both figures.

Discussion

The following section starts with summing up the results of the experiment and its conclusions for RDW algorithms. Afterwards, limitations of the methods are presented. The discussion is concluded with prospects for future research and applications.

Hypotheses

H1: Because the exposure to a constant rightward curvature gain resulted in an increased perceptual threshold for rightward curvature gains at two days, H1 can be confirmed. After approximately 20 minutes of adaptation, the threshold was shifted from 0.1 m^{-1} to 0.14 m^{-1} . The resulting perceptual thresholds allow decreasing the radius from 10.2 m to 6.97 m. The radius could not be further decreased substantially after the Second Adaptation (7.16 m), indicating saturation effects of the applied curvature gain during adaptation.

H2: After adaptation to a rightward curvature gain, subjects walked significantly more rightwards when asked to walk in a straight line, without visual feedback, so H2 can be confirmed. After the First Adaptation, subjects walked 0.2 m further to the right than in the Baseline condition. Although the effect was not present on the next day in the Carry-Over condition, the finding could be replicated after the Second Adaptation (0.53 m). Interestingly, the effect was significantly bigger the second time. Moreover, the walking paths show that subjects walked on a curvy line after adaptation.

H3: After adaptation to a rightward curvature gain, subjects did not point to significantly different directions, when asked to point straight, without visual feedback of their hands, so H3 has to be rejected.

H4: Changes of the rightward threshold were significantly different from the Baseline even one day after the adaptation. From the First Adaptation to the Carry-Over condition, the threshold shifted from 0.14 m^{-1} to 0.13 m^{-1} . The resulting perceptual thresholds mean a slightly increasing radius from 6.97 m to 7.78 m, which is still significantly smaller than the Baseline (10.2 m). Interestingly, the slope of both conditions directly after the adaptation (First Adaptation = 3.5, Second Adaptation = 3.42) were steeper than the slope of the Baseline (2.81). This was not the case in the Carry-Over condition (2.84), indicating that the psychometric curves retained the shifted threshold even one day after the adaptation, while the PSE shifted back to the Baseline.

To our knowledge, this is the first time an adaptation effect could be shown in a RDW experiment. This result offers a lot of opportunities for developing more efficient RDW algorithms, since the maximum curvature gain can be imperceptibly increased after adaptation. It may even be possible to increase the effect by using continuously bigger curvature gains during the adaptation phase. Ultimately this approach could allow users to walk in a circle in room-sized physical spaces, while perceiving an unlimited VE. Since the slope of the threshold function was significantly different before and after adaptation, it seems that subjects did not accept a broader range of curvatures, but instead perceived a different set of curvature gains as straight forward directly after adaptation. However, one day later, the PSE shifted back, while the heightened threshold remained at its adapted position. The exposure to the real world led to a deadaptation of the straight walking behaviour. Since in natural walking scenarios one is often rotating to a target and walking straight instead of walking on a curved path, the subjects may have deadapted less at the perceptual threshold.

Limitations

Our results show that the exposure to a curvature gain leads to adaptation effects in perception and walking behaviour. However, there are some questions that could not be answered by the current experiment:

Adaptation to Complex Algorithms. In our experiment, we used a very simple curvature gain algorithm that was using constant gains instead of correcting the gain value dependent on the room position or the walking speed of the subject. This might make our results not directly applicable to more complex RDW algorithms that were used in the past. We would assume that the adaptation process is different, when a more complex algorithm is used and would argue that it needs to be tested how different parameters, like dynamically changing the strength of the curvature gain, influence the adaptation process. Additionally, the same principle might be usable for rotational and translational gains as well, maybe even a multi-adaptation process to complex algorithms is possible.

However, we proved that an adaptation to one side to a specific gain is possible in a setting where the user is walking from one target to another. This means that through adaptation, a more efficient use of the physical space can be achieved. After this adaptation, the perceptual effect can of course be used in a setting with a position-dependent one-sided RDW algorithm, with a stronger curvature gain.

We did only adapt to one side during the experiment and it remains unknown if an adaptation to two opposite gains would lead to a two-sided effect resulting in psychometric functions with lower slopes or if both sides compensate each other. However, we would argue that using a one-sided RDW algorithm together with adaptation might outperform its two-sided equivalent. Moreover, since in natural walking scenarios one is often rotating

to a target and walking straight afterwards, one-sided algorithms are applicable in most scenarios.

The Influence of Walking Speed. Since we allowed subjects to choose a natural walking speed and the different conditions did not show systematic speed differences, we could not quantify possible effects of the walking speed on adaptation. The small difference that was found for the Carry-Over condition might result from it being the first part of the third experimental session. Because walking speed was identified to influence the perceptual threshold without adaptation (Neth et al., 2012), we believe that this topic should be examined in future experiments.

Fitting of the Psychometric Curves. After inspecting the data of subject 3 and 9, we would assume that answers to the 2AFC-like task may have been given confusing leftward and rightward gains. Since the fitting package was set to fit a monotonic uprising psychometric curve, the tested parameters could only vary in a given ratio and a flat curve was fitted for these subjects. Although no criteria for data quality was defined before the experiment, the two subjects were excluded from the described analysis, since the fitted parameters would not have been reasonably based on the given data (see Appendix 4). However, even including them did not change the results in a significant way.

Pointing Task. The results of this experiment indicate that adaptation had no effect on pointing of the subjects. The average pointing direction of the different conditions did not vary in a systematic way. However, in all measurements, the data shows that subjects pointed slightly to the left. Additionally, high standard deviations were present in all conditions. Since the position tracking of the HMD was turned off (to track the controller during the pointing process) it was possible that subjects changed their position during the pointing task. Such a behaviour would not be detectable in the

data and would lead to a wrong interpretation. To heighten the quality of the obtained data, the position of the controller and the HMD should both be tracked at the same time in future experiments. However, this problem could have occurred in all conditions, but since no systematic difference was found between the conditions, we would suggest that adaptation to a curvature gain did indeed not change pointing behaviour without visual feedback of the hand. The reason for this result in comparison to Kitazawa, Kimura, and Uka (1997) may be that during our adaptation task, subjects did not see their hands. Since behaviours like reaching or pointing seem to be error driven (Shadmehr et al., 2010), adaptation may not have been able to have an effect, since in contrast to prism glass studies, no visual error between the hand and the target was perceivable in our task. Until now, it remains an open question if an effect of adaptation to a curvature gain can be achieved if the pointing hand is shown in the VE.

Orientation Data. To measure the effects of curvature gains that are applied over time, it is crucial to track orientation accurately. When we noticed slight drifts in orientation over time during pretesting, we decided to realign the HMD to the tracking space after every trial. To gain more information for future experiments, we collected data of a second orientation tracker in all sessions. The slopes calculated from the collected data of the HMD and the InertiaCube 3 during the experiment showed that the mean orientation of both devices was slightly increasing over time. However, since we only tested one sensor of each type, these results may not be representative. Nevertheless, we would highly suggest to realign in short intervals whenever using curvature gains.

Prospects

Although this work is a first step in making use of adaptation processes in RDW, there are some topics that need to be investigated to make use of it in future applications:

- 1. Cost and Reward:** Since the perceptual threshold did not shift any further after the second adaptation, we would assume a saturation effect, like those conducted in other adaptation contexts (e.g. saccadic adaptation (Hopp & Fuchs, 2004)). It remains an open question if a stronger curvature gain would allow even bigger shifts of the perceptual threshold. On the other hand, even an adaptation block with less trials might have been sufficient to achieve the same result. We would argue that the investigation of the initial adaptation process over time would be an interesting topic considering cost and reward of adapted redirected walking.
- 2. Motion sickness:** After the experimental sessions, subjects reported that symptoms of motion sickness appeared during the threshold blocks. The questionnaire results of this study indicate that simulator sickness became smaller as participants became more experienced with the VE and being adapted. This fits the idea of motion sickness as a result of diverging sensory input. But to fit psychometric curves, we also needed to test strong curvature gains to find stimuli that were unambiguous. However, for entertainment applications motion sickness should be minimized. So guidelines for VE that consider possible parameters and their influence on motion sickness during adaption should be developed.
- 3. Cognitive load:** Point & Teleport and RDW have both been identified to influence cognitive processes during its application (Bowman et al., 1997; Bruder et al., 2015). On the one hand, a VE should be highly transferable into the real world,

so cognitive tasks should of course influence virtual walking. On the other hand, additional effects like lower performance in spatial awareness should be reduced. A question that should be answered in the future is, whether adaptation is a possibility to reduce the cognitive load of redirected walking.

4. Immersion: The level of details and the resulting immersion might play a role in the detectability of gains (Peck et al., 2009) and this factor might also interfere with the adaptation process. For future research, a systematic variation of this factor during adaptation should be considered. Moreover, it would be helpful to define universal and precise variables to measure and compare the level of details or the latent factor immersion between different scenarios.

5. Consequences of adaptation: Lastly, we would like to point out that the short-term consequences of adaptation to RDW are still unknown and should be investigated. Our results show that effects persisted at least one day after the experiment. On the one hand, this leads to interesting opportunities for entertainment applications because a regular user would need less adaptation phases. On the other hand, the perceptual shifts might alter a subject's behaviour in the real world (e.g. traffic) and might be a potential safety risk that needs to be evaluated carefully in the future.

References

- Alahyane, N., & Pélisson, D. (2005). Long-lasting modifications of saccadic eye movements following adaptation induced in the double-step target paradigm. *Learning & Memory, 12*(4), 433–443.
- Bates, D., Mächler, M., Bolker, B., & Walker, S. (2015). Fitting linear mixed-effects models using lme4. *Journal of Statistical Software, 67*(1), 1–48. doi: 10.18637/jss.v067.i01
- Bolte, B., de Lussanet, M., & Lappe, M. (2016). Virtual reality system for the enhancement of mobility in patients with chronic back pain. *Int J Child Health Hum Dev, 9*(3), 305.
- Bolte, B., & Lappe, M. (2015). Subliminal reorientation and reposition in immersive virtual environments using saccadic suppression. *IEEE Transactions on Visualization and Computer Graphics, 21*, 545 – 552.
- Bowman, D. A., Koller, D., & Hodges, L. F. (1997). A methodology for the evaluation of travel techniques for immersive virtual environments. *Journal of the Virtual Reality Society, 3*, 120–131.
- Bozgeyikli, E., Raij, A., Katkooi, S., & Dubey, R. (2016). Point & teleport locomotion technique for virtual reality. In *Proceedings of the 2016 annual symposium on computer-human interaction in play* (pp. 205–216). New York, NY, USA: ACM. Retrieved from <http://doi.acm.org/10.1145/2967934.2968105> doi: 10.1145/2967934.2968105
- Bruder, G., Interrante, V., Phillips, L., & Steinicke, F. (2012, April). Redirecting walking and driving for natural navigation in immersive virtual environments. *IEEE Transactions on Visualization and Computer Graphics, 18*(4), 538-545. doi:

10.1109/TVCG.2012.55

Bruder, G., Lubos, P., & Steinicke, F. (2015, April). Cognitive resource demands of redirected walking. *IEEE Transactions on Visualization and Computer Graphics*, *21*(4), 539-544. doi: 10.1109/TVCG.2015.2391864

Bruder, G., Steinicke, F., Hinrichs, K., & Lappe, M. (2009). Reorientation during Body Turns. In M. Hirose, D. Schmalstieg, C. A. Wingrave, & K. Nishimura (Eds.), *Joint virtual reality conference of egve - icat - eurovr*. The Eurographics Association. doi: 10.2312/EGVE/JVRC09/145-152

Friedman, M. (1937). The use of ranks to avoid the assumption of normality implicit in the analysis of variance. *Journal of the American Statistical Association*, *32*(200), 675-701. Retrieved from <https://www.tandfonline.com/doi/abs/10.1080/01621459.1937.10503522> doi: 10.1080/01621459.1937.10503522

Grechkin, T., Thomas, J., Azmandian, M., Bolas, M., & Suma, E. (2016). Revisiting detection thresholds for redirected walking: Combining translation and curvature gains. In *Proceedings of the acm symposium on applied perception* (pp. 113–120). New York, NY, USA: ACM. Retrieved from <http://doi.acm.org/10.1145/2931002.2931018> doi: 10.1145/2931002.2931018

Hedges, L., & Olkin, I. (1985). *Statistical models for meta-analysis*. New York: Academic Press.

Hodgson, E., Bachmann, E., & Waller, D. (2008, December). Redirected walking to explore virtual environments: Assessing the potential for spatial interference. *ACM Trans. Appl. Percept.*, *8*(4), 22:1–22:22. Retrieved from <http://doi.acm.org/10.1145/2043603.2043604> doi: 10.1145/2043603.2043604

Hopp, J., & Fuchs, A. F. (2004). The characteristics and neuronal substrate

- of saccadic eye movement plasticity. *Progress in Neurobiology*, 72(1), 27 - 53. Retrieved from <http://www.sciencedirect.com/science/article/pii/S030100820300193X> doi: <https://doi.org/10.1016/j.pneurobio.2003.12.002>
- Interrante, V., Ries, B., & Anderson, L. (2007, 01). Seven league boots: A new metaphor for augmented locomotion through moderately large scale immersive virtual environments. *3D User Interfaces*, 0, null. doi: 10.1109/3DUI.2007.340791
- Jerald, J., Whitton, M., & Brooks, F. P., Jr. (2012, March). Scene-motion thresholds during head yaw for immersive virtual environments. *ACM Trans. Appl. Percept.*, 9(1), 4:1–4:23. Retrieved from <http://doi.acm.org/10.1145/2134203.2134207> doi: 10.1145/2134203.2134207
- Kalman, R. E. (1960). A new approach to linear filtering and prediction problems. *Transactions of the ASME—Journal of Basic Engineering*, 82(Series D), 35–45.
- Kennedy, R. S., Lane, N. E., Berbaum, K. S., & Lilienthal, M. G. (1993). Simulator sickness questionnaire: An enhanced method for quantifying simulator sickness. *The International Journal of Aviation Psychology*, 3(3), 203-220. doi: 10.1207/s15327108ijap0303\3
- Kitazawa, S., Kimura, T., & Uka, T. (1997). Prism adaptation of reaching movements: Specificity for the velocity of reaching. *Journal of Neuroscience*, 17(4), 1481–1492. Retrieved from <http://www.jneurosci.org/content/17/4/1481> doi: 10.1523/JNEUROSCI.17-04-01481.1997
- Kuznetsova, A., Brockhoff, P. B., & Christensen, R. H. B. (2017). lmerTest package: Tests in linear mixed effects models. *Journal of Statistical Software*, 82(13), 1–26. doi: 10.18637/jss.v082.i13
- Langbehn, E., Lubos, P., Bruder, G., & Steinicke, F. (2017, April). Bending the curve:

- Sensitivity to bending of curved paths and application in room-scale vr. *IEEE Transactions on Visualization and Computer Graphics*, 23(4), 1389-1398. doi: 10.1109/TVCG.2017.2657220
- Langbehn, E., & Steinicke, F. (2018). Redirected walking in virtual reality. In *Springer encyclopedia of computer graphics and games* (p. 1-11).
- Larrue, F., Sauzeon, H., Wallet, G., Foloppe, D., Cazalets, J.-R., Gross, C., & N’Kaoua, B. (2014). Influence of body-centered information on the transfer of spatial learning from a virtual to a real environment. *Journal of Cognitive Psychology*, 26(8), 906-918. Retrieved from <https://doi.org/10.1080/20445911.2014.965714> doi: 10.1080/20445911.2014.965714
- MATLAB. (2018). *version 9.5.0.942161 (r2018b)*. Natick, Massachusetts: The MathWorks Inc.
- Nescher, T., Huang, Y.-Y., & Kunz, A. (2014, March). Planning redirection techniques for optimal free walking experience using model predictive control. In *2014 IEEE Symposium on 3d User Interfaces (3DUI)* (p. 111-118). doi: 10.1109/3DUI.2014.6798851
- Neth, C. T., Souman, J. L., Engel, D., Kloos, U., Bulthoff, H. H., & Mohler, B. J. (2012, July). Velocity-dependent dynamic curvature gain for redirected walking. *IEEE Transactions on Visualization and Computer Graphics*, 18(7), 1041-1052. doi: 10.1109/TVCG.2011.275
- Nguyen, A., Rothacher, Y., Lenggenhager, B., Brugger, P., & Kunz, A. (2018). Individual differences and impact of gender on curvature redirection thresholds. In *Proceedings of the 15th ACM symposium on applied perception* (pp. 5:1–5:4). New York, NY, USA: ACM. Retrieved from <http://doi.acm.org/10.1145/3225153.3225155>

doi: 10.1145/3225153.3225155

Nogalski, M., & Fohl, W. (2017). Curvature gains in redirected walking: A closer look. In *2017 IEEE Virtual Reality (VR)* (Vol. 00, p. 267-268). Retrieved from doi: [.ieeecomputersociety.org/10.1109/VR.2017.7892279](https://doi.org/10.1109/VR.2017.7892279) doi: 10.1109/VR.2017.7892279

Peck, T. C., Fuchs, H., & Whitton, M. C. (2009, May). Evaluation of reorientation techniques and distractors for walking in large virtual environments. *IEEE Transactions on Visualization and Computer Graphics*, *15*(3), 383-394. doi: 10.1109/TVCG.2008.191

Peck, T. C., Whitton, M. C., & Fuchs, H. (2008). Evaluation of reorientation techniques for walking in large virtual environments. In *Ieee virtual reality* (p. 121-127).

Prism Game Studios Ltd. (2016, May). *Portal stories: Vr*. Prism Game Studios Ltd.

R Core Team. (2013). R: A language and environment for statistical computing [Computer software manual]. Vienna, Austria. Retrieved from <http://www.R-project.org/> (ISBN 3-900051-07-0)

Razzaque, S., Kohn, Z., & Whitton, M. (2001). Redirected walking. In *Proceedings of the ACM Eurographics conference* (pp. 289-294).

Schütt, H. H., Harmeling, S., Macke, J. H., & Wichmann, F. A. (2016). Painfree and accurate bayesian estimation of psychometric functions for (potentially) overdispersed data. *Vision Research*, *122*, 105 - 123. Retrieved from <http://www.sciencedirect.com/science/article/pii/S0042698916000390> doi: <https://doi.org/10.1016/j.visres.2016.02.002>

Shadmehr, R., Smith, M. A., & Krakauer, J. W. (2010). Error correction, sensory prediction, and adaptation in motor control. *Annual Review of Neuroscience*, *33*(1), 89-

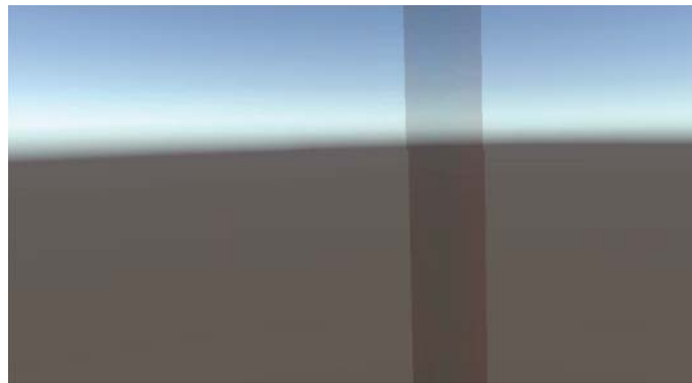
108. Retrieved from <https://doi.org/10.1146/annurev-neuro-060909-153135>
(PMID: 20367317) doi: 10.1146/annurev-neuro-060909-153135
- Shapiro, S. S., & Wilk, M. B. (1965). An analysis of variance test for normality (complete samples). *Biometrika*, *52*(3/4), 591–611. Retrieved from <http://www.jstor.org/stable/2333709>
- Steinicke, F., Bruder, G., Hinrichs, K., Jerald, J., Frenz, H., & Lappe, M. (2009). Real walking through virtual environments by redirection techniques. *JVRB - Journal of Virtual Reality and Broadcasting*, *6*(2009)(2). Retrieved from <http://nbn-resolving.de/urn:nbn:de:0009-6-17472> doi: 10.20385/1860-2037/6.2009.2
- Steinicke, F., Bruder, G., Jerald, J., Frenz, H., & Lappe, M. (2010, Jan). Estimation of detection thresholds for redirected walking techniques. *IEEE Transactions on Visualization and Computer Graphics*, *16*(1), 17-27. doi: 10.1109/TVCG.2009.62
- Suma, E. A., Clark, S., Krum, D., Finkelstein, S., Bolas, M., & Warte, Z. (2011, March). Leveraging change blindness for redirection in virtual environments. In *2011 IEEE Virtual Reality Conference* (p. 159-166). doi: 10.1109/VR.2011.5759455
- Sun, Q., Patney, A., Wei, L., Shapira, O., Lu, J., Asente, P., ... Kaufman, A. E. (2018). Towards virtual reality infinite walking: dynamic saccadic redirection. *ACM Trans. Graph.*, *37*(4), 67:1–67:13.
- Tseng, Y.-w., Diedrichsen, J., Krakauer, J. W., Shadmehr, R., & Bastian, A. J. (2007). Sensory prediction errors drive cerebellum-dependent adaptation of reaching. *Journal of Neurophysiology*, *98*(1), 54-62. Retrieved from <https://doi.org/10.1152/jn.00266.2007> (PMID: 17507504) doi: 10.1152/jn.00266.2007
- Unity Technologies. (2017). *Unity*. San Francisco, California , U.S. Retrieved from unity3d.com

- Usoh, M., Catena, E., Arman, S., & Slater, M. (2000). Using presence questionnaires in reality. *Presence: Teleoperators and Virtual Environments*, 9(5), 497-503. Retrieved from <https://doi.org/10.1162/105474600566989> doi: 10.1162/105474600566989
- Wilcoxon, F. (1945). Individual comparisons by ranking methods. *Biometrics Bulletin*, 1(6), 80–83. Retrieved from <http://www.jstor.org/stable/3001968>
- Williams, B., Narasimham, G., P. McNamara, T., Carr, T., J. Rieser, J., & Bodenheimer, B. (2006, 01). Updating orientation in large virtual environments using scaled translational gain. In (p. 21-28). doi: 10.1145/1140491.1140495

Appendix

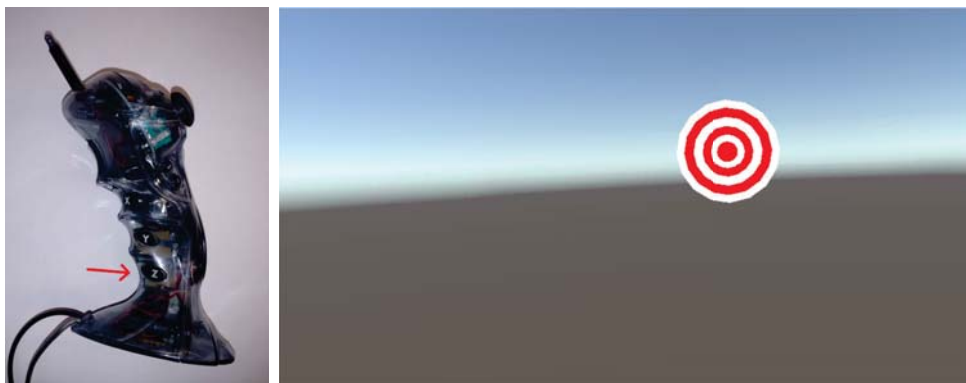
A1: Instructions

1) Sie befinden sich in einer leeren virtuellen Welt. Gehen Sie zunächst zu der roten Säule.

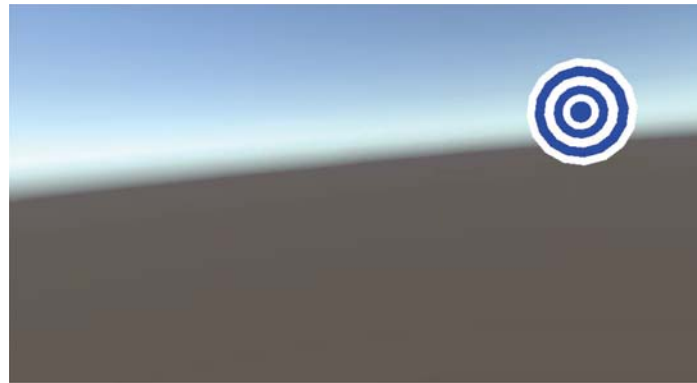


2) Sobald Sie in der Säule stehen ertönen zwei Pieptöne, bitte bleiben Sie währenddessen stehen.

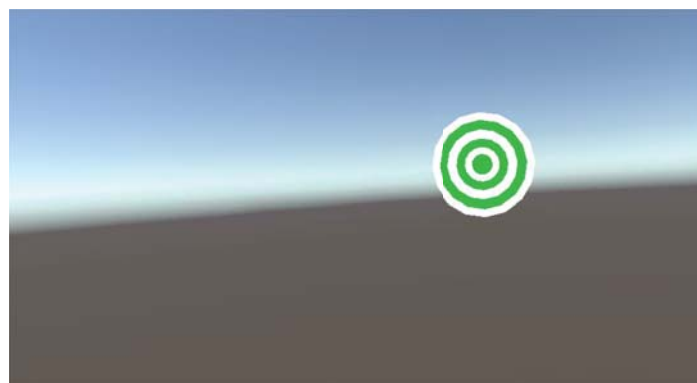
3) Nun erscheint eine rote Zielscheibe. Bitte drücken Sie nun die Z-Taste auf dem Controller und zeigen sie in Richtung des Ziels. Es ertönt ein Klickgeräusch.



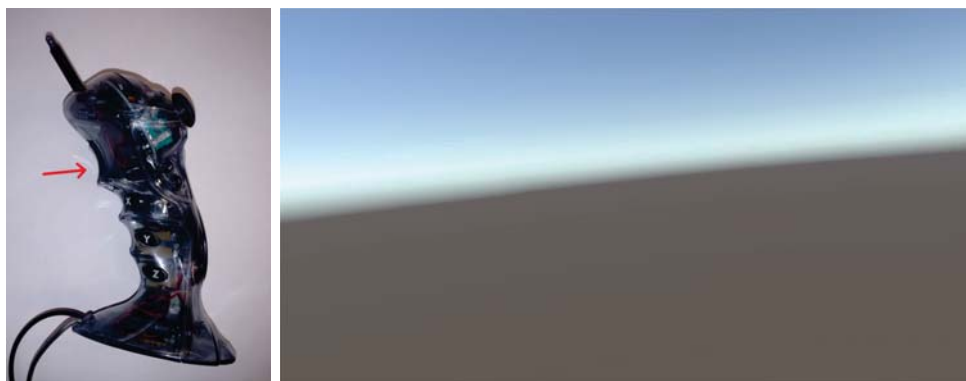
4) Lassen Sie nun die Z Taste los, das Ziel sollte nun blau sein.



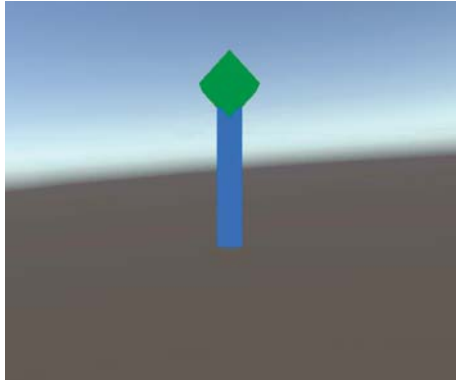
5) Bitte schauen Sie auf das Ziel, das Ziel sollte nun grün sein.



6) Schießen Sie nun mit der Trigger-Taste auf die Zielscheibe. Diese sollte nun verschwinden.

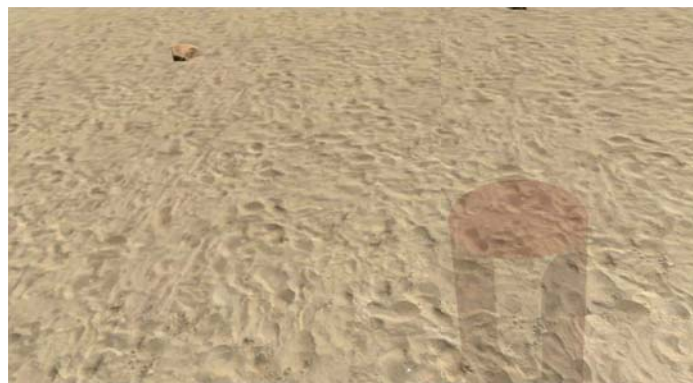


7) Bitte gehen Sie geradeaus in Richtung des Ziels, sobald dieses verschwunden ist und bleiben Sie stehen, sobald sie einen Pfeil sehen.

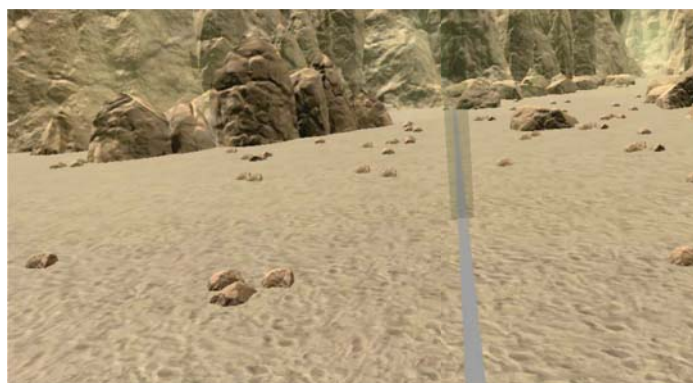


8) Bitte drehen Sie sich nun um und begeben Sie sich zurück zur roten Säule, es folgen nun mehrere Durchgänge dieser Art.

9) Nach einigen Durchläufen werden Sie sich in einer Wüstenlandschaft wiederfinden, sobald Sie die rote Säule erreicht haben.



10) Bitte folgen Sie nun möglichst genau dem weißen Pfad auf dem Boden. Um genau auf diesem Weg zu gehen, müssen Sie in der realen Welt einen Halbkreis nach rechts oder links laufen. Das Ende des Weges ist durch eine weitere Säule gekennzeichnet:



11) Sobald dieser erreicht wird, erscheint in einigen Durchgängen ein Auswahlmenü.

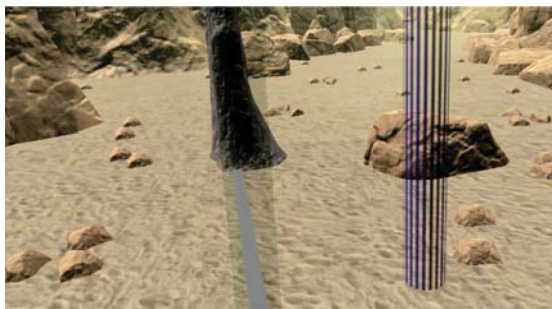


12) Erscheint das Menü, müssen Sie entscheiden, ob Sie eine linke oder rechte Kreisbahn gelaufen sind. Die Auswahl erfolgt mit den A-, B-, C-Buttons des Controllers. Falls Sie sich nicht sicher sind, entscheiden Sie sich bitte für die Seite, die Ihnen wahrscheinlicher vorkommt.



13) Im oberen Bereich Sichtfeld wird eine Punktzahl angezeigt: Diese gibt an, wie genau Sie auf dem Pfad gelaufen sind. Die Bewertung reicht dabei von 0 bis 100 Punkten. Rechts daneben steht die Gesamtpunktzahl.

14) Nach einigen Durchgängen wird eine gestreifte Säule erscheinen. Sollten Sie keine weiteren Fragen haben, können Sie diese betreten um die Testläufe zu beenden und das eigentliche Experiment zu starten.



Während des ganzen Experiments besteht keine Gefahr in etwas hineinzulaufen. Sollten Sie sich einer Wand zu sehr nähern, erscheint sofort eine Warnung im Programm, wodurch das Sichtfeld komplett rot wird. Bitte bleiben Sie in diesem Fall stehen.



A2: Curvature Gain

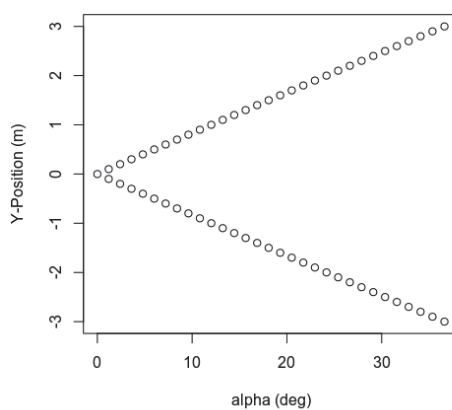


Figure 19. Simulated α -values for $\lambda = 0$, $r = 4,77$ m and the subject walking on an ideal path.

A3: Straight Walking & Pointing Task

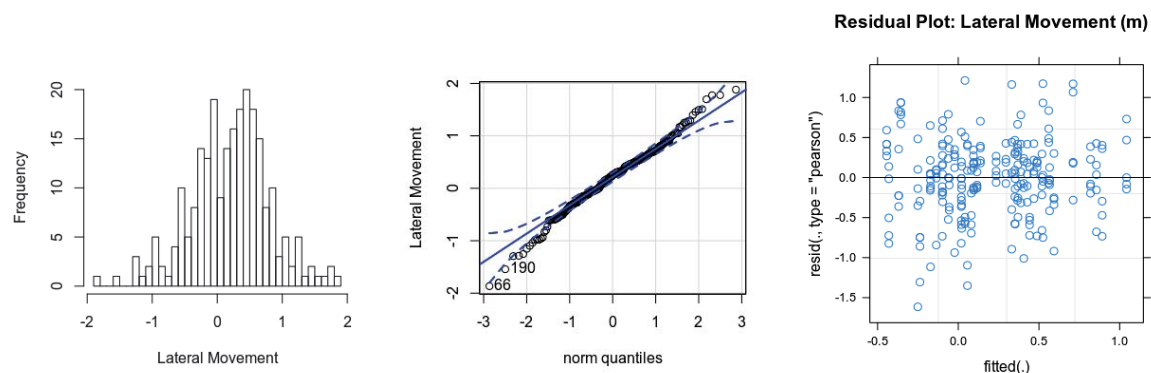


Figure 20. Histogram, QQ-plot and residual plot of the lateral walking movements during the straight walking task.

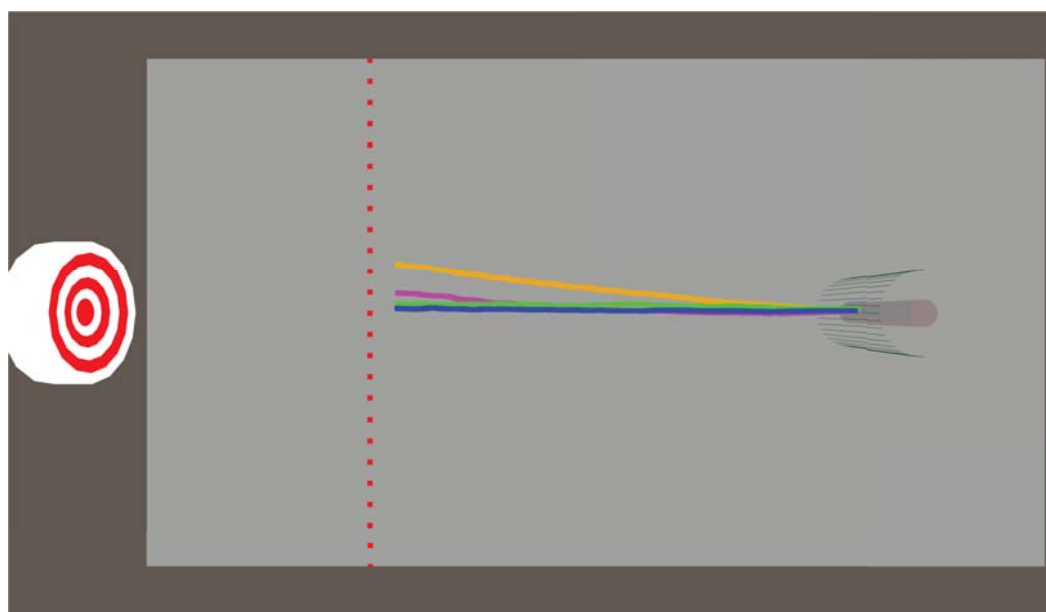


Figure 21. Averaged and filtered walking paths mapped into the VE. Baseline (blue) and Carry-Over (green) seem to be straight forward, while First Adaptation (magenta) and Second Adaptation (orange) show lateral movements in direction of the curvature gain.

A4: Threshold Measurement

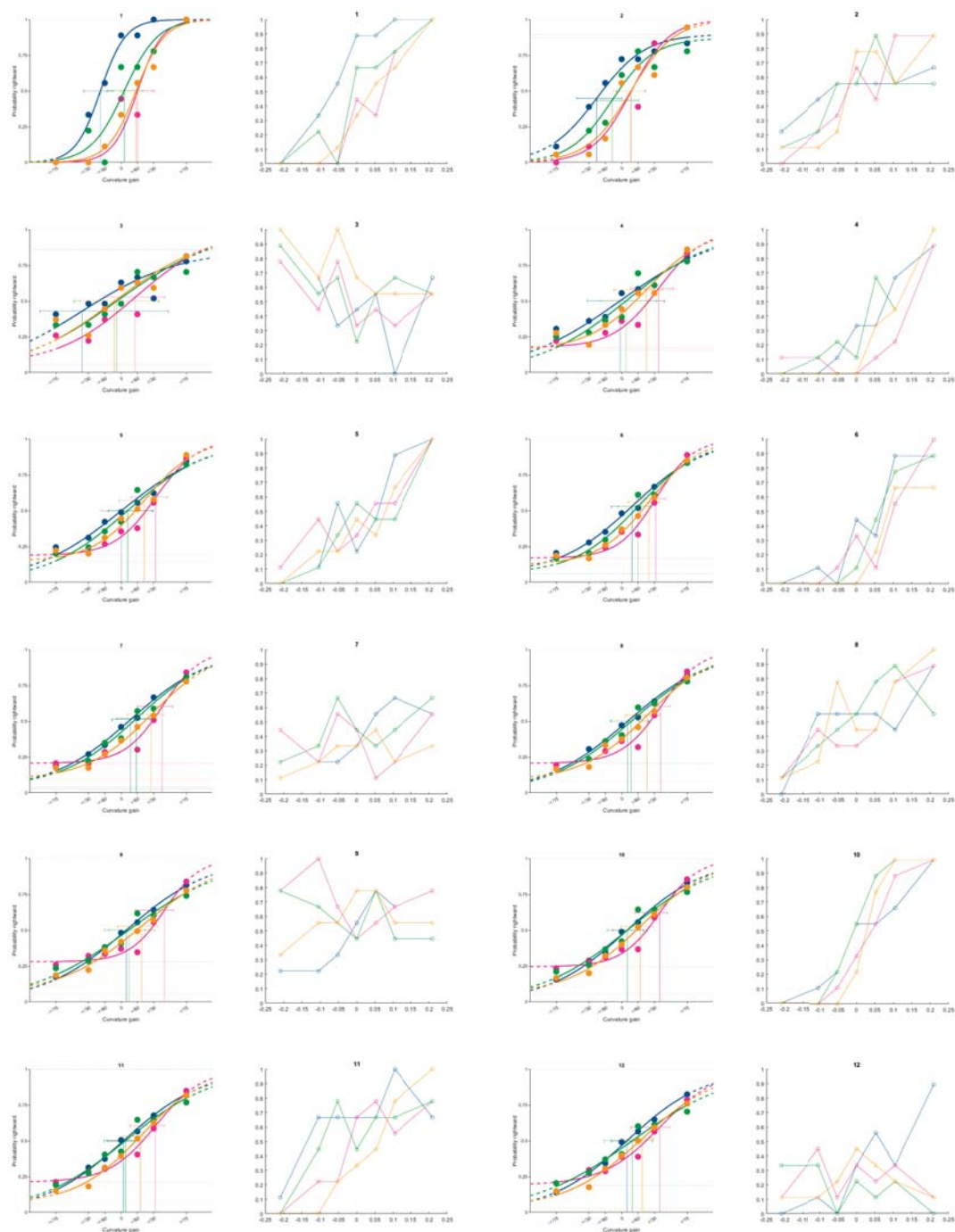


Figure 22. Raw data and single fits of all subjects. Subject 3 and Subject 9 were excluded because subjects seemed to have answered the wrong way round. Error bars indicate .95 confidence intervals for the PSE of the specific subject in this condition (Baseline (blue), First Adapt (magenta), Carry-Over (green), Second Adapt (orange)).

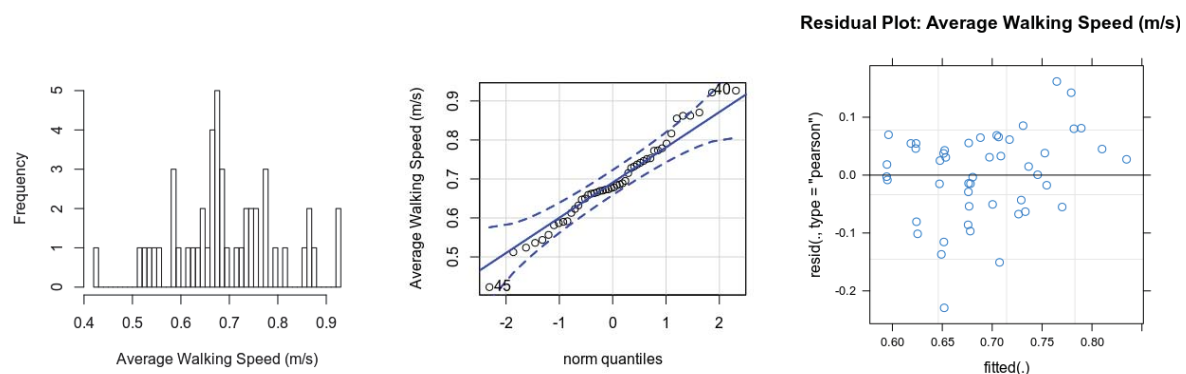


Figure 23. Histogram, QQ-plot and residual plot of the average walking speed from the Threshold Measurements.

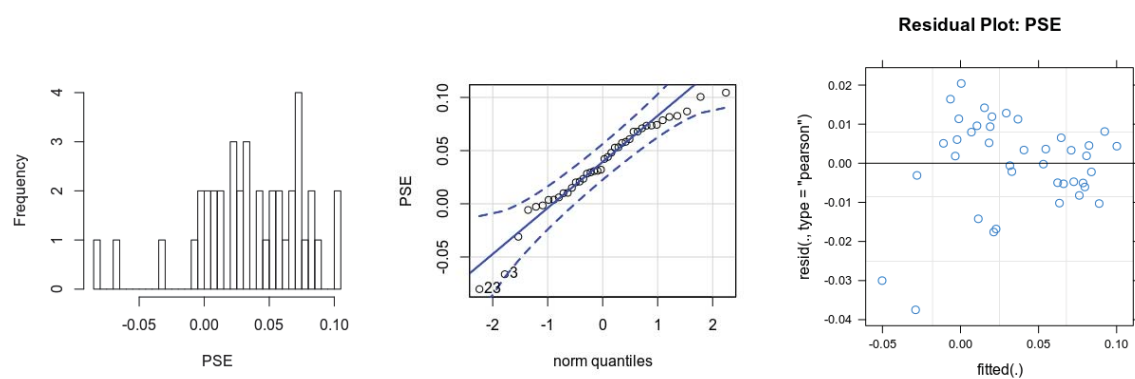


Figure 24. Histogram, QQ-plot and residual plot of the PSEs from the fitted curves.

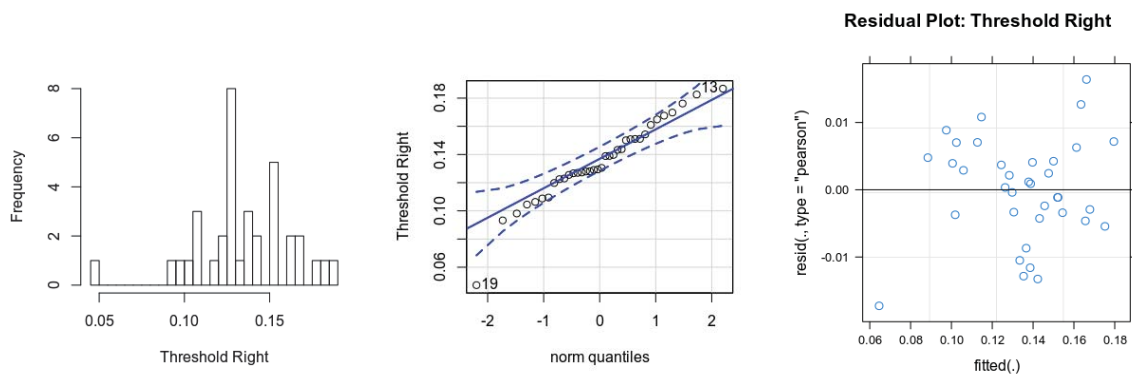


Figure 25. Histogram, QQ-plot and residual plot of the 75%-Thresholds from the fitted curves.

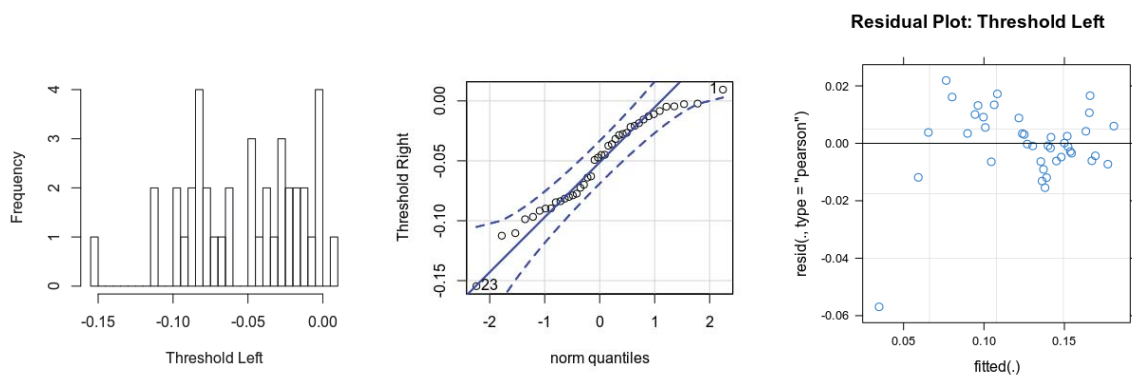


Figure 26. Histogram, QQ-plot and residual plot of the 25%-Thresholds from the fitted curves.

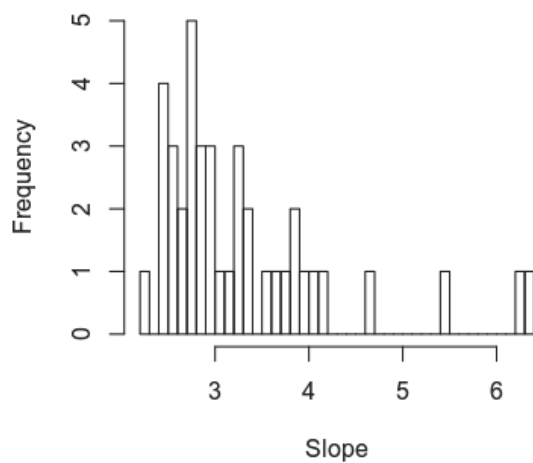


Figure 27. Histogram of the resulting slopes from the fitted psychometric curves.

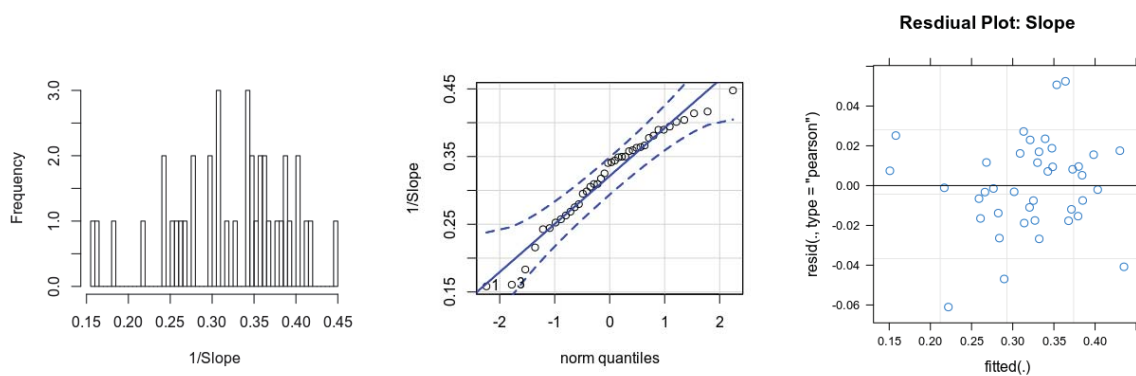


Figure 28. Histogram, QQ-plot and residual plot of the inverse Slopes from the fitted curves.

Table 2. Mean values of PSE and thresholds of all four conditions.

Parameter	Condition	1/radius (m^{-1})	radius (m)	gC	Hedges' g
PSE	Baseline	0.006025215	165.97	521.41	
	First Adaptation*	0.075818242	13.19	41.44	2.6
	Carry-Over* ⁺ [⊥]	0.016310882	61.31	192.61	0.69
	Second Adaptation* ⁺	0.059536167	16.80	52.77	2.25
75%-Threshold	Baseline	0.09799437	10.20	32.06	
	First Adaptation*	0.14337956	6.97	21.91	1.09
	Carry-Over* ⁺ [⊥]	0.12861702	7.78	24.43	0.72
	Second Adaptation*	0.13966711	7.16	22.49	1.01
25%-Threshold	Baseline	-0.09954899	-10.05	-31.56	
	First Adaptation*	-0.01828872	-54.68	-171.78	3.87
	Carry-Over* ⁺ [⊥]	-0.06993047	-14.30	-44.92	1.48
	Second Adaptation*	-0.0211685	-47.24	-148.41	4.01

Note. Negative values can be interpreted as leftward curvature. * indicate a significant difference from the Baseline, ⁺ a significant difference from the First Adaptation and [⊥] a significant difference from the Second Adaptation condition. Hedges' g was calculated in comparison to the Baseline condition.

Table 3. Slopes of all four conditions.

	1/Slope	Slope	Hedges' g
Baseline	0.3565008	2.805043	
First Adaption*	0.2854704	3.50299	0.98
Carry-Over ^{+⊥}	0.3515583	2.844479	0.07
Second Adaptation*	0.2926928	3.416552	0.94

Note. * indicate a significant difference from the Baseline, ⁺ a significant difference from the First Adaptation and [⊥] a significant difference from the Second Adaptation condition. Hedges' g was calculated in comparison to the Baseline condition

Acknowledgements

I would like to thank: Prof. Dr. Markus Lappe, Dr. Annegret Meermeier, Luke Bölling, Steffen Flagge, Phil Wieland, Kerstin Richert, Gianni Bremer, Lena Kegel, Milena Merkel, Hannah Lettmann, Birgit Liesenklas, all employees of the technical service of the psychology department at the Westfälische Wilhelms-Universität Münster and all participants who took part in the experiments.

Plagiatserklärung

Hiermit versichere ich, dass die vorliegende Arbeit "Shifting Perception: Adaptation to a Curvature Gain in Redirected Walking" selbstständig verfasst worden ist, dass keine anderen Quellen und Hilfsmittel als die angegebenen benutzt worden sind und dass die Stellen der Arbeit, die anderen Werken - auch elektronischen Medien - dem Wortlaut oder Sinn nach entnommenen wurden, auf jeden Fall unter Angabe der Quelle als Entlehnung kenntlich gemacht worden sind.

_____ (Datum, Unterschrift)

Ich erkläre mich mit einem Abgleich der Arbeit mit anderen Texten zwecks Auffindung von Übereinstimmungen sowie mit einer zu diesem Zweck vorzunehmenden Speicherung der Arbeit in eine Datenbank einverstanden.

_____ (Datum, Unterschrift)